U.S.N.A. --- Trident Scholar project report; no. 435 (2015)

A THEORETICAL AND EXPERIMENTAL ANALYSIS OF POST-COMPRESSION WATER INJECTION IN A ROLLS-ROYCE M250 GAS TURBINE ENGINE

by

Midshipman 1/C Brian R. He
United States Naval Academy
Annapolis, Maryland

_____
(signature)

Certification of Adviser(s) Approval

Professor Martin R. Cerza
Mechanical Engineering Department

_____
(signature)

_____
(date)

Acceptance for the Trident Scholar Committee

Professor Maria J. Schroeder
Associate Director of Midshipman Research

_____
(signature)

_____
(date)

USNA-1531-2

REPORT DOCUMENTATION PAGE

Form Approved
OMB No. 0704-0188

1. REPORT DATE *(DD-MM-YYYY)*	**2. REPORT TYPE**	**3. DATES COVERED** *(From - To)*
05-18-2015		

4. TITLE AND SUBTITLE
A Theoretical and Experimental Analysis of Post-Compression Water Injection in a Rolls-Royce M250 Gas Turbine Engine

5a. CONTRACT NUMBER

5b. GRANT NUMBER

5c. PROGRAM ELEMENT NUMBER

6. AUTHOR(S)
He, Brian Ray

5d. PROJECT NUMBER

5e. TASK NUMBER

5f. WORK UNIT NUMBER

7. PERFORMING ORGANIZATION NAME(S) AND ADDRESS(ES)

8. PERFORMING ORGANIZATION REPORT NUMBER

9. SPONSORING / MONITORING AGENCY NAME(S) AND ADDRESS(ES)
U.S. Naval Academy
Annapolis, MD 21402

10. SPONSOR/MONITOR'S ACRONYM(S)

11. SPONSOR/MONITOR'S REPORT NUMBER(S)
Trident Scholar Report no. 435 (2015)

12. DISTRIBUTION / AVAILABILITY STATEMENT

This document has been approved for public release; its distribution is UNLIMITED.

13. SUPPLEMENTARY NOTES

14. ABSTRACT

The gas turbine engine is one of the most common methods of energy generation and propulsion used by the military today due to its high power-to-weight ratio and ability to operate using a wide variety of fuels. Spurred by ongoing concerns regarding air pollution from energy generation sources, researchers have explored numerous systems for reducing gas turbine emissions and improving efficiency. One of these systems involves spraying water into the gas turbine in order to improve power output and reduce nitric oxide concentration. This project investigates the effects on power output, efficiency, operating conditions, and emissions of injecting water at the compressor discharge of a Rolls-Royce M250.

The results indicated that post-compression water injection can increase engine power output for a specific combustor temperature at the cost of increased fuel consumption. At a flow rate of 0.8 gpm, injecting water at the compressor discharge yielded a 17% increase in net power over the baseline at the 100% throttle setting. Post-compression water injection also significantly reduced the nitric oxide emissions at the expense of an increase in unburned hydrocarbon concentration. The 0.8 gpm flow rate produced a 50% reduction in NO_x from the baseline at 100% throttle. Since injecting water at the compressor discharge avoids exposing the compressor to liquid water droplets, post-compression water injection could be used as an alternative to inlet fogging in low pressure-ratio gas turbines.

15. SUBJECT TERMS
gas turbines, water injection, emissions reduction, turbine augmentation methods, nitric oxides

16. SECURITY CLASSIFICATION OF:			**17. LIMITATION OF ABSTRACT**	**18. NUMBER OF PAGES**	**19a. NAME OF RESPONSIBLE PERSON**
a. REPORT	**b. ABSTRACT**	**c. THIS PAGE**		81	**19b. TELEPHONE NUMBER** *(include area code)*

Standard Form 298 (Rev. 8-98)
Prescribed by ANSI Std. Z39.18

Abstract

The gas turbine engine is one of the most common methods of energy generation and propulsion used by the military today. Its applications include surface ships, aircraft, and tanks, and it is highly regarded due to its high power-to-weight ratio and ability to operate using a wide variety of fuels. Spurred by ongoing concerns regarding air pollution from energy generation sources, researchers have explored numerous systems for reducing gas turbine emissions and improving efficiency. One of these systems involves spraying water into the gas turbine in order to improve power output and reduce nitric oxide concentration.

Water injection is typically implemented in one of two ways: post-compression water injection, which involves spraying at either the combustion chamber or compressor discharge; or compressor inlet fogging, which entails spraying water at the inlet of the engine. Previous research has examined the effects of the two water injection methods on high pressure-ratio gas turbines, such as the LM2500, as well as the effects of compressor inlet fogging on low pressure-ratio gas turbines, such as the Rolls-Royce M250. However, there are few conclusive results regarding the use of post-compression water injection on low pressure-ratio gas turbines. The project investigates the effects on power output, efficiency, operating conditions, and emissions of injecting water at the compressor discharge of a Rolls-Royce M250.

Experimental runs with seven different water flow rates ranging from 0.1 to 0.8 gpm were conducted using an original spray assembly on one of USNA's Rolls-Royce M250 gas turbine engines. All seven flow rates were tested with water at 15ºC, with additional tests conducted at 45ºC and 60ºC for the 0.4 gpm and 0.6 gpm flow rates. The effects of varying the temperature and flow rate of the injected water were examined based on measured brake horsepower, torque, operating temperatures and pressures, and emissions concentrations. Experimental results were compared with data from a previous compressor inlet fogging project using the same model gas

turbine engine.

The results indicated that post-compression water injection can increase engine power output for a specific combustor temperature at the cost of increased fuel consumption. At a flow rate of 0.8 gpm, injecting water at the compressor discharge yielded a 17% increase in net power over the baseline at the 100% throttle setting. Post-compression water injection also significantly reduced the nitric oxide emissions at the expense of an increase in unburned hydrocarbon concentration. The 0.8 gpm flow rate produced a 50% reduction in NO_x from the baseline at 100% throttle.

Results of increasing the water temperature by sensible preheating of the water before injection yielded no significant effects on engine performance and emissions. Comparison of normalized results for post-compression water injection and inlet fogging on power output, brake specific fuel consumption, and combustor temperature generally indicated that inlet fogging and water injection produced comparable effects on engine performance. Since injecting water at the compressor discharge avoids exposing the compressor to liquid water droplets, post-compression water injection could be used as an alternative to inlet fogging in low pressure-ratio gas turbines.

Keywords

Gas turbines, water injection, emissions reduction, turbine augmentation methods, nitric oxides

Acknowledgements

I would like to thank my research advisor, Professor Martin Cerza, for his continued help and support throughout the last four years as both his student and advisee. Additionally, I would like to thank Mr. Charles Baesch and Mr. Charlie Popp from the Engineering and Weapons Department Technical Support Division for their advice and assistance in all aspects of construction, operation, and data collection. Without them, especially Mr. Baesch, completion of this project would not have been possible. Additionally, I would like to thank the USNA Machine Shop for assisting me in fabrication of the parts needed to construct my project assembly. Lastly, I would like to thank the Trident Scholar Committee and the Office of Naval Research for providing me with this excellent opportunity to pursue my interests and take advantage of the bountiful academic resources that the Naval Academy has to offer.

Table of Contents

List of Figures and Tables

List of Figures

List of Tables

1. INTRODUCTION

Since its development in the 1930s, the gas turbine has been one of the most common methods of power production today and is currently utilized in ships, trains, tanks, aircraft, and power plants across the world. It is advantageous because it can produce a large amount of power for its relatively small weight and can be used with a wide variety of fuels [1]. Advancements to the gas turbine have been developed to make it more efficient and environmentally-friendly. Implementing these advancements in marine gas turbine systems could help the Navy accomplish its goals for energy and environmental security [2].

One of these advancements, water injection, involves spraying water mist into a gas turbine engine. Water injection is a method of increasing the power output and decreasing greenhouse gas emissions of gas turbine engines [3]. While water injection is not a new concept, it appears that little research has compared the effect of different water injection techniques on the performance and emissions of low pressure ratio gas turbine engines [4]. The project will compare the results of post-compression water injection on the Rolls-Royce Model 250 to those of inlet fogging systems on the same engine model. It will also investigate the effects of heating different water flow rates with regard to engine performance and emissions.

2. BACKGROUND

2.1. Gas Turbine Engines

A basic gas turbine engine is comprised of a compressor, a combustion chamber, one or more turbines, and a heat rejection process. In this project, an open-cycle gas turbine will be used, meaning that the engine takes in the working fluid from the environment and rejects it back to the environment at the end of the cycle. A schematic of a basic open cycle gas turbine engine is shown in Figure 1.

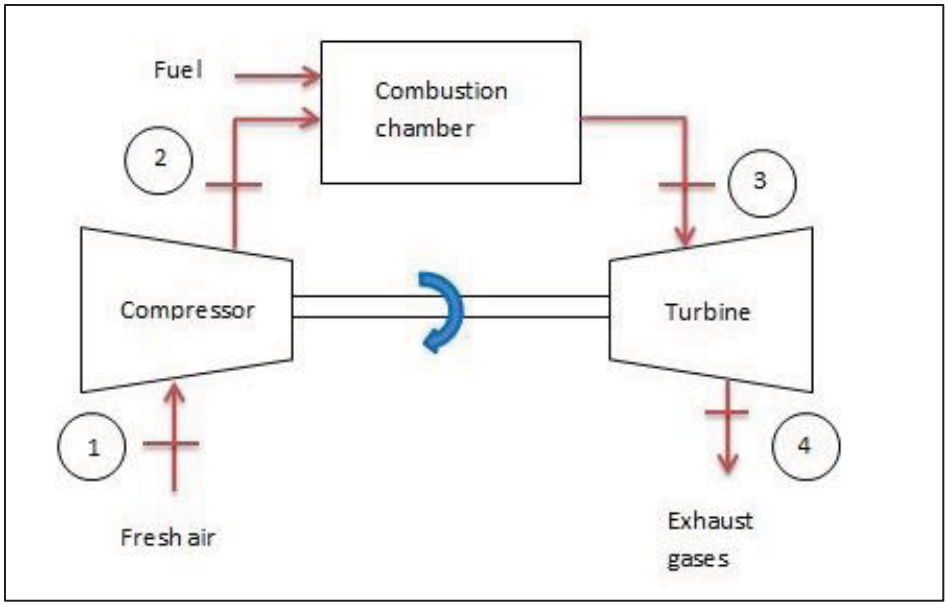

Figure 1: Schematic of Open Cycle Gas Turbine

An open cycle gas turbine can be modeled using an ideal cycle called the Brayton Cycle. A temperature versus entropy (T-s) diagram for the Brayton Cycle can be found in Figure 2. The thermodynamic state points shown in Figure 2 correspond to the same physical locations indicated in Figure 1.

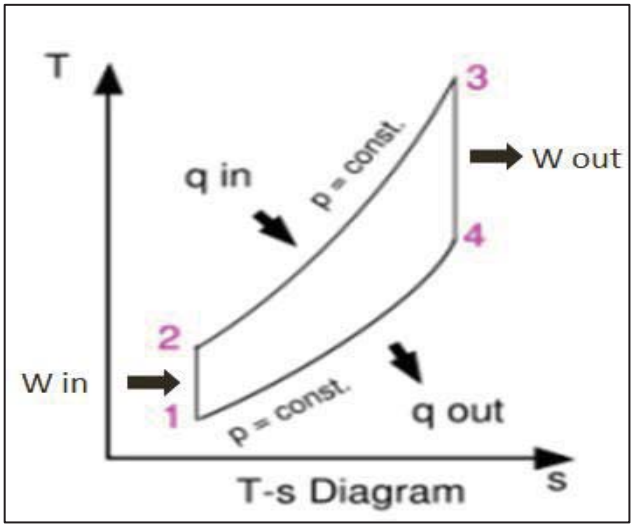

Figure 2: T-s diagram of Brayton Cycle

In typical open-cycle gas turbine engines, air first enters the compressor, where it is pressurized and heated. This process is represented by the increase in temperature and pressure

between state points 1 and 2 in Figure 2. As Figure 2 demonstrates, the compression process requires work and the ratio of the pressure at point 2 compared to at point 1 is called the pressure ratio. After passing through the compressor, the pressurized air is combined with a fuel in the combustion chamber and burned at approximately constant pressure. The air temperature subsequently increases and chemical reaction products are generated. This air and product mixture is represented by state 3 in Figure 2 and the isobaric combustion process that created the mixture is represented by the transition between points 2 and 3 in Figure 2. After combustion, the high-temperature air mixture passes through turbines, where it expands and produces shaft work. This expansion process is represented by the decrease in temperature and pressure between states 3 and 4 shown in Figure 2. The process from state 4 back to state 1 represents the isobaric rejection of heat in the exhaust back to atmospheric conditions in an open-cycle gas turbine.

In a split-shaft gas turbine engine, such as the Naval Academy's Rolls-Royce Model 250, the expansion of the air mixture generates power through turbines on two spools: a gas generator turbine (compressor turbine) and a power turbine. The gas generator turbine is connected to the compressor on the same shaft and produces the power needed to operate the compressor and any auxiliary requirements of the gas turbine. After passing through the gas generator turbine, the air expands through the power turbine and produces useful power for propulsion or electricity generation. A schematic of a typical split-shaft gas turbine engine is shown in Figure 3 and a photograph of the Naval Academy's Rolls-Royce M250, with relevant parts labeled, is shown in Figure 4.

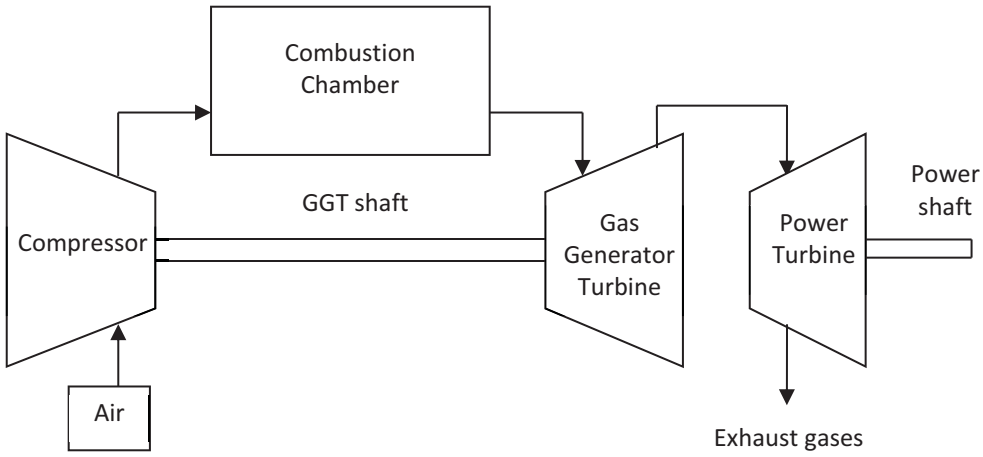

Figure 3: Schematic of typical turboshaft gas turbine engine

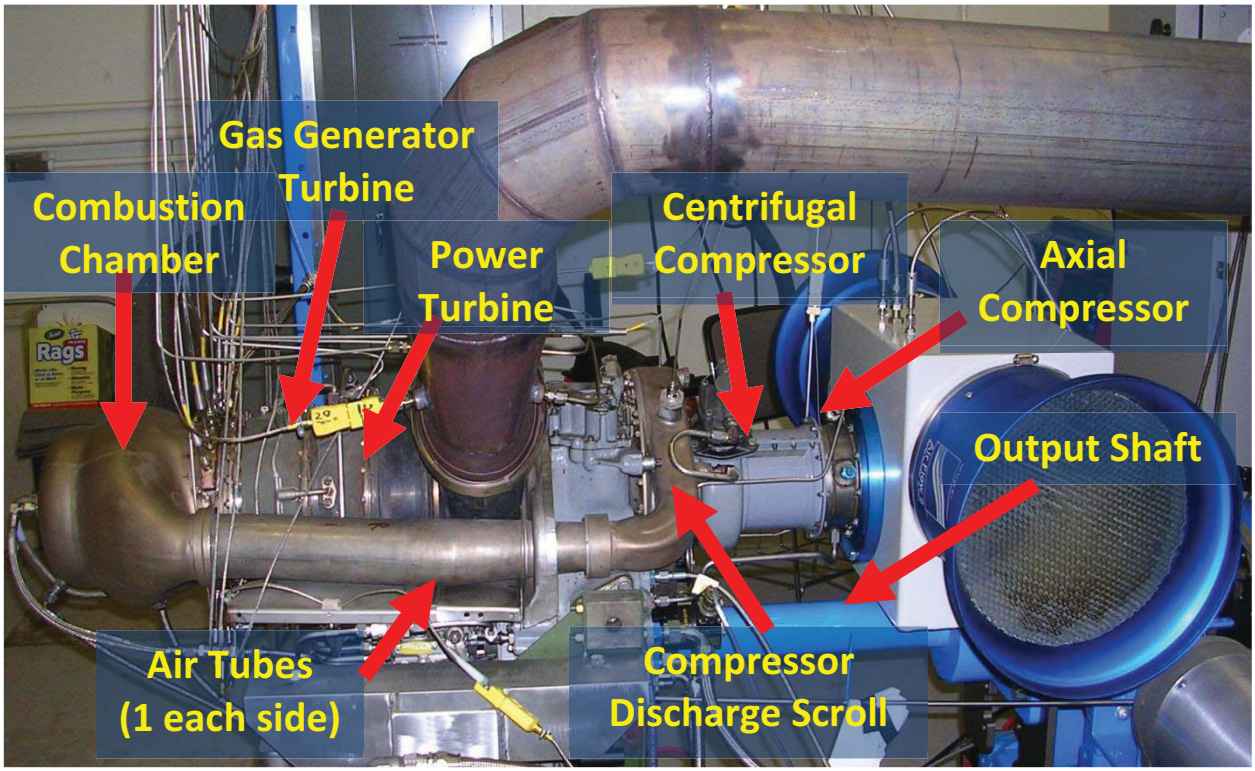

Figure 4: RR-M250 with parts labeled

The addition of the gas generator turbine to the open cycle gas turbine changes the representative temperature-entropy diagram for the system. An additional work extraction process occurs after combustion that provides at least as much work as is needed to operate the compressor. As a result, the power that can be generated from the power turbine decreases

compared to the same engine cycle without the gas generator turbine stage. A temperature versus entropy plot of a split-shaft system operating under isentropic conditions is shown in Figure 5.

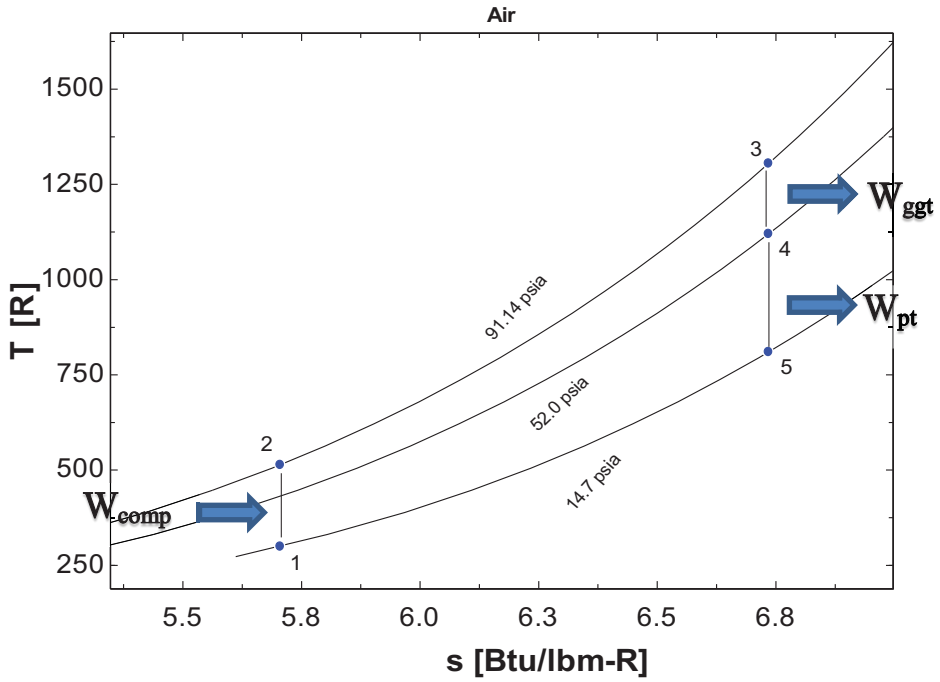

Figure 5: Temperature v. entropy diagram for split-shaft gas turbine

In Figure 5, the process occurring between state points 3 and 4 represents the work extracted by the gas generator turbine. State point 4 is an intermediate point between the gas generator turbine and power turbine stages. Since part of the total work potential through both turbines is extracted by the gas generator turbine to power the compressor and auxiliary engine demands, the work that the power turbine is capable of performing decreases as the work that the gas generator turbine performs increases. Thus, if the compressor required less work, the gas generator turbine would correspondingly perform less work and the net work performed by the power turbine would increase.

2.2. Water Injection History

Gas turbine engines have undergone many advancement and augmentation methods since they began being widely used. Water injection is a well-known aviation technology that was

originally used decades ago to increase engine power during takeoff [5]. It has since been used in popular aircraft such as the Boeing 707-120 and 747-100/200. As aircraft engines became more powerful, water injection was no longer needed in aircraft and instead began to be more widely used in land-based industrial turbines to decrease the concentrations of unwanted emissions. Water and steam injection are currently used in many land-based gas turbine applications today to help control emissions levels, specifically those of nitric oxides (NO_x) and carbon monoxide (CO), to within acceptable limits regulated by government policy.

2.3. Compressor Inlet Fogging

Water injection can be incorporated into gas turbines in several ways. One method, known as inlet fogging, involves spraying water at the turbine inlet. This method increases the power output of the gas turbine by cooling the inlet air, thereby reducing the work that the compressor performs on the air. Water sprayed at the compressor inlet evaporates during the compression process, causing the temperature of the inlet air to decrease. Reducing the inlet temperature causes the air density to increase when compared to a no-spray system, which in turn implies a decrease in specific volume (v). For a compression process, the specific work required to pressurize the air and water mixture is a function of its specific volume, as shown in Equation 1 [6]. Equation 1 indicates that decreasing the specific volume of the inlet air through inlet fogging causes a corresponding decrease in required compressor work. The negative value indicates that the process requires work rather than performs it.

$$w_{comp} = -\int v \, dP \qquad \text{(Equation 1)}$$

For a turboshaft gas turbine engine, such as the Rolls-Royce Model 250, the reduction in compressor work caused by inlet fogging in turn requires less work from the gas generator turbine. As Figure 5 previously indicated, for a fixed combustor exit temperature, a reduction in

the work extracted through the gas generator turbine means there is more available energy for the power turbine. As a result, the net specific work produced by the engine increases with inlet fogging. If the total mass flow rate through the engine remains constant, compressor inlet fogging will increase the net power output from the turbines.

Since inlet fogging reduces the required compressor power while increasing the power output, the resulting increase in net power can allow an overall increase in cycle thermal efficiency. Injecting water into the cycle increases the heat rate, and thus fuel, needed for combustion at a fixed power output level. This increase in heat rate occurs because some of the energy in the combustion process that would have otherwise been used to heat the air is used to vaporize the water droplets. However, if inlet fogging can increase the net power to a greater magnitude than the increase in heat rate, the thermal efficiency can increase. Equation 2 shows the equation for thermal efficiency.

$$\eta_{th}\ (thermal\ efficiency) = \frac{\dot{W}_{net}}{\dot{Q}_{in}} \qquad \text{(Equation 2)}$$

Figure 6 shows a schematic of a turboshaft gas turbine with compressor inlet fogging.

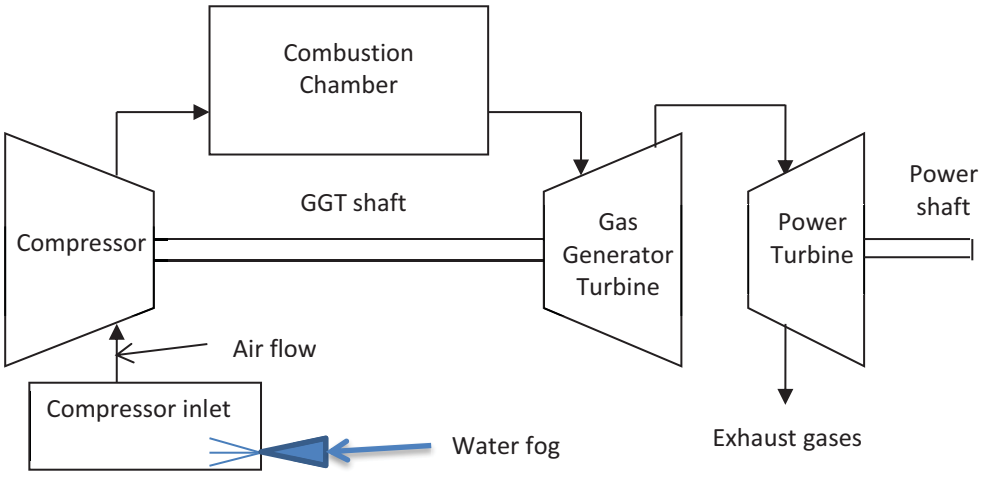

Figure 6: Schematic of inlet fogging system on turboshaft gas turbine

2.4. Post-compression Water Injection

Spraying water into either the combustion chamber or directly after the compressor is the other primary method of water injection for gas turbine performance augmentation. Since this water injection technique bypasses the compressor, it does not affect the compressor work. Rather, post-compression water injection relies on increasing the power output by increasing the mass flowing through the power turbine. The addition of water vapor to the air causes the total mass flow rate through the power turbine to increase. Equation 3 demonstrates how increasing the mass flow rate can increase power turbine output. The equation for the power output of the power turbine is derived from the First Law of Thermodynamics for open systems.

$$\dot{W}_{pt} = (\dot{m}_a + \dot{m}_w)(\Delta h_{mix}) \quad \text{(Equation 3)}$$

The addition of the water mass and energy to the total fluid mass and energy flowing through the turbine increases the net power from the turbines.

Despite improving power output, water injection at the compressor discharge can cause the overall thermal efficiency of the cycle to decrease. Due to the cooling effect of water entering the cycle, the amount of fuel energy needed to heat the working fluid up to the combustor conditions for a specified engine power increases. As previously shown in Equation 2, thermal efficiency is defined as the ratio of the net power to the rate of heat input. Water injection at the compressor discharge can potentially increase the heat rate to a greater degree than the increase in power and cause the thermal efficiency to decrease. Since the heat is provided by combustion of fuel, the engine would consequently use more fuel than when operating without water injection. The project aims to determine whether the theoretical increase in power output caused by water injection can actually be observed in the Rolls-Royce M250, and what effects the water spray will actually have on the efficiency and emissions concentrations.

2.5. Steam Augmentation

If the injected water is pre-heated until it forms steam, water injection turns into a process called steam augmentation [7]. Steam augmentation adds mass to the air in the form of water vapor, but unlike in water injection, heat from the combustion process is not used to vaporize liquid water. As a result, most of the energy from the combustor flame is used directly to heat the product gases. If the steam has a high enough temperature, its addition to the compressor discharge airstream could produce an air-steam mixture with a higher energy than that of the existing air. This increased energy could reduce the heat rate needed to increase the temperature of the product gases and thereby increase thermal efficiency. Since the heat is supplied by the addition of fuel, less fuel would be required to heat the gases in the combustor to achieve a desired power output. Despite its benefits, steam augmentation is currently primarily limited to use in land-based power plants due to the large amount of energy required to superheat the water to the desired temperatures.

2.6. Emissions Effects

Inlet fogging, water injection, and steam augmentation all have similar effects on emissions. Injecting water into the engine reduces the combustor temperature, which decreases the amount of thermal nitric oxides (NO_x) produced by the combustion reaction. At the same time, decreasing the combustor temperature increases the amount of unburned hydrocarbons and carbon monoxide [8]. Ideally, the combustor temperature should be maintained so that a low level of nitric oxides, carbon monoxide, and unburned hydrocarbons can be achieved. Figure 7 displays the general relationship between combustor temperature and emissions.

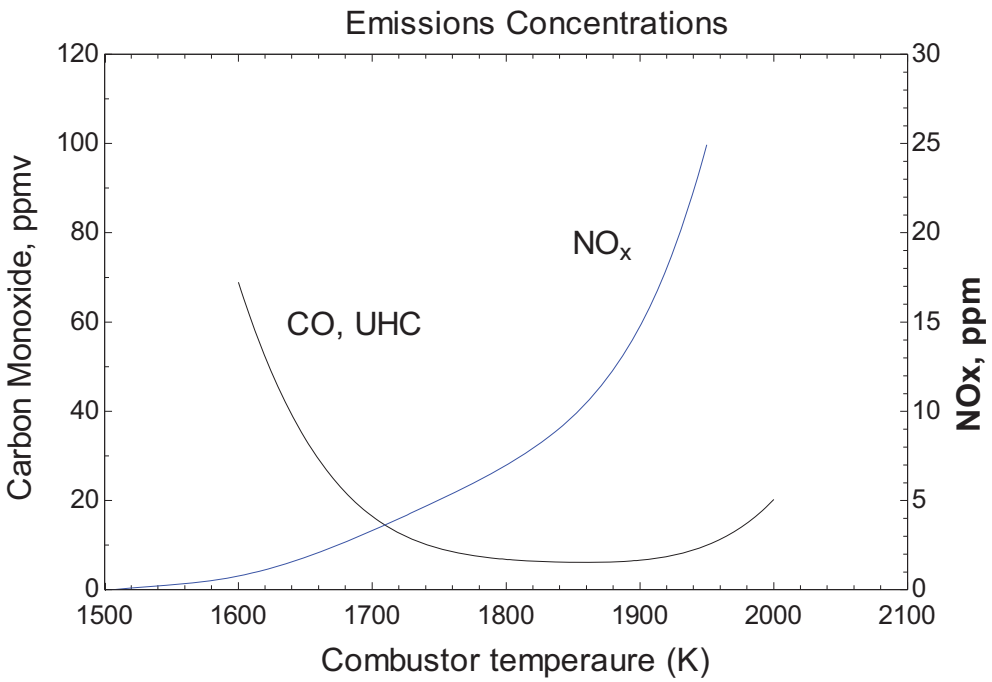

Figure 7: General relationship between combustor temperature and emissions

The ideal temperatures at which the combustor should operate for minimum emissions are near the intercept of the two curves representing the different emissions relationships. Cooling the combustor through water injection allows the gas turbine to operate closer to optimum conditions for emissions reduction.

3. RESEARCH OBJECTIVES

3.1. Rationale for Study

While it poses appealing benefits to power output, efficiency, and emissions, inlet fogging can pose increased hazards to the gas turbine because water is being injected upstream of the compressor. If the water droplets do not completely evaporate prior to entering the compressor, the liquid impacting the compressor blades could negatively affect its long-term operation. While both inlet fogging and post-compression water injection have similar effects on the life of the hot-section turbine parts, Klaus Brun and Rainer Kurtz found that inlet fogging can

reduce compressor component life when combined with other factors relating to turbine operation [9].

Furthermore, according to studies conducted by a joint group of researchers from Boeing, Rolls-Royce, and NASA, the amount of water needed to reduce NO_x emissions through water injection methods is less for post-compression water injection than for compressor inlet fogging. In their studies, the researchers investigated the amount of water needed to achieve a certain level of NO_x reduction in a large aeroderivative gas turbine engine. Each test was conducted during takeoff up to an altitude of 3,000 feet. In order to achieve a 65% NO_x reduction by injecting water after the compressor, the water flow rate needed ranged from 14,750 to 19,830 lb/hr/engine. For compressor inlet fogging, the water flow rate needed to achieve a 50% reduction engine ranged from 26,265-31,340 lb/hr/engine. Thus, using post-compression water injection to reduce NO_x emissions allowed the engine to operate with over a 60% reduction in water flow rate when compared with the flow rate needed for inlet fogging to achieve the same effect [10].

In industrial applications, concern for engine life often requires the water used for injection or inlet fogging to be at least boiler quality in terms of impurities [11]. The reduced flow rate requirement for post-compression injection would decrease the rate of energy input into water treatment systems compared to that of inlet fogging applications. Additionally, inlet fogging provides the largest benefits in primarily hot, low-humidity climates and can even cause icing of the compressor if used at ambient temperatures too far below 59ºF (15ºC) [12]. Water injected after the compression stage of the gas turbine stage bypasses the compressor and can be employed in all climates.

Sensible heating of the water prior to injection can potentially reduce the heat rate and

fuel energy required to heat the air-water mixture when compared with the no-heat condition. If heating of the water is conducted through a means that does not require additional heat input, such as waste-heat recovery, the overall cycle thermal efficiency can return to no-spray levels. Most importantly, comparison of the results of inlet fogging with those of post-compressor water injection can yield relationships that may assist in determining the best water injection implementation options for future gas turbine systems. Relationships between the techniques can be used towards research in marine gas turbine applications.

3.2. Objectives

Inlet fogging was explored in a previous project, Trident Report #367, which investigated the effects of inlet fogging on low pressure-ratio gas turbines such as the Naval Academy's Rolls-Royce Model 250 [13]. The objective of this research project was to evaluate the effects of post-compressor water injection on the same model of gas turbine engine and compare the effects of the two different water injection methods with regard to power, efficiency, and emissions. Additionally, the project will investigate the effects of pre-heating the injected water with regard to the gas turbine performance metrics. These objectives will be achieved through the fabrication of a heating and water injection assembly located at the compressor discharge scroll of a Rolls-Royce Model 250-C20B Turboshaft gas turbine engine. The water will be pre-heated and pressurized before being sprayed at different flow rates into the engine. A theoretical thermodynamic model will be developed using the Engineering Equation Solver™ program (EES™) to predict the performance of the Rolls-Royce Model 250. The performance parameters for the model will include net power produced, cycle thermal efficiency, and brake specific fuel consumption. Results from the theoretical calculations will be used to guide the experimentation process and the experimental data will be used in the final

analysis of post-compression water injection as well as any comparisons with compressor inlet fogging.

4. THEORETICAL ANALYSIS

4.1. Assumptions

The thermodynamic model of the water injection configuration developed using EES™ can be found in Appendix A. The EES™ code includes several assumptions regarding the water spray and mixing process. Two of these assumptions governed the pressure before and after water injection in the gas turbine cycle. One assumption stated that the partial pressure of the air would remain constant after the water was injected, causing the total pressure to increase. The second assumption stated that the total pressure would remain constant before and after injection, thereby implying that the partial pressure of the air would decrease. Results of the model using each of the assumptions regarding the mixture pressure were obtained and then compared to identify any significant differences between the two approaches.

The combustion chamber was also assumed to be adiabatic while turbine and compressor efficiencies were assumed to be consistent with values calculated from previous tests on the gas turbine engine. Air was treated as an ideal gas and the power produced by the gas generator turbine was assumed to be equal to the compressor power. Lastly, the engine was assumed to be operating under steady-state conditions and kinetic and potential energy effects were assumed to be negligible.

4.2. Cycle Analysis with Water Injection

For the purpose of analysis, each component of the open-cycle gas turbine was considered an open system bounded by individual control volumes. An energy rate balance could then be obtained for each component based on the First Law of Thermodynamics. The complete energy

balance is shown in Equation 4. The subscripts denote inlet (i) and exit (e) properties of the fluid flow within the control volume.

$$\frac{dE_{CV}}{dt} = \dot{Q} - \dot{W}_{CV} + \dot{m}_i\left(h_i + \frac{{v_i}^2}{2} + gz_i\right) - \dot{m}_e\left(h_e + \frac{{v_e}^2}{2} + gz_e\right) \qquad \text{(Equation 4)}$$

Using the assumptions regarding steady-state conditions with negligible differences in kinetic and gravitational potential energy, the heat rate and power can be expressed as the product of the mass flow rates and changes in specific enthalpy, as shown in Equations 5 and 6. These equations also assume conservation of mass within the control volume.

$$\dot{W}_{CV} = \dot{m}\,(h_i - h_e),\ when\ \dot{Q} = 0 \qquad \text{(Equation 5)}$$

$$\dot{Q} = \dot{m}\,(h_i - h_e),\ when\ \dot{W}_{CV} = 0 \qquad \text{(Equation 6)}$$

The theoretical calculations used equations similar to Equations 5 and 6 to determine all the power produced and required by the engine as well as the heat rates into the combustor and out to the atmosphere. These performance metrics were calculated using temperatures and pressures at various state points in the cycle. If mass flow rate of the air, water, and fuel are known and data is provided regarding the shaft speed, torque and emissions, performance and emissions metrics can be determined for any gas turbine configuration. Analyzing a gas turbine cycle necessitates examining the thermodynamic conditions at each state point and their implications for the different metrics used to measure gas turbine performance. A schematic of a split-shaft gas turbine with post-compression water injection is shown in Figure 8 to identify the various thermodynamic state points used in the analysis. The nomenclature for the actual state points used in the EES™ code in Appendix A differed slightly from what is shown for simplicity in Figure 8.

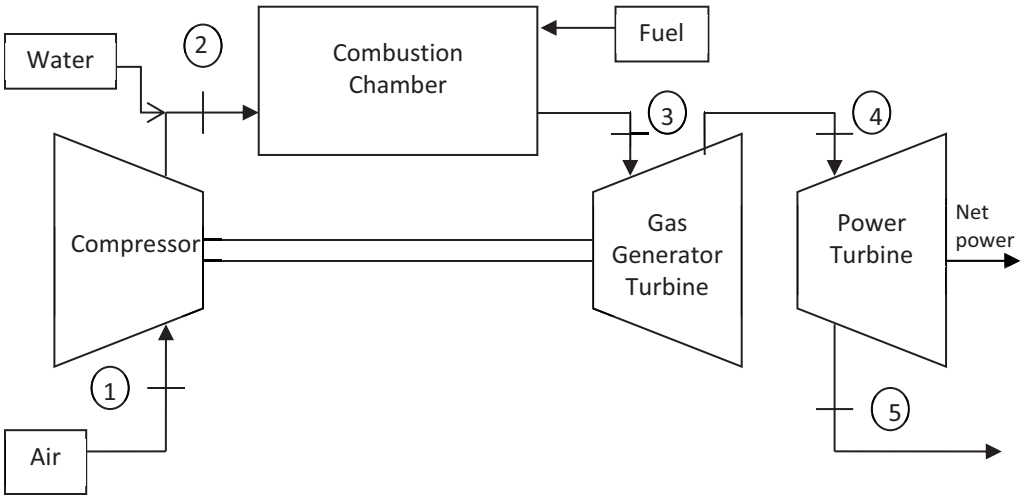

Figure 8: Schematic of split-shaft gas turbine with water injection

Starting at the compressor inlet (point 1), the air enters the turbine cycle at atmospheric conditions and is compressed to a greater pressure and temperature. The inlet enthalpy and entropy can be calculated using the known ambient temperature and pressure. Once these values are determined, the temperatures and pressures at state point 2 after the compressor can be calculated using the ideal, isentropic values for the process given the pressure ratio of the turbine. The compressor efficiency is used to determine the actual enthalpy of the air at state point 2, which is solely a function of temperature under the ideal gas assumption. The equation for isentropic efficiency is shown in Equation 7, where "a" represents the actual value and "s" represents the isentropic value. The difference in enthalpies is equal to the specific work.

$$\eta_{comp} = \frac{w_s}{w_a} = \frac{h_{2,s} - h_1}{h_{2,a} - h_1} \qquad \text{(Equation 7)}$$

After the compression stage, the air is mixed with water and the resulting pressure is equal to the sum of the partial pressures of the air and the water once it exits the nozzle. Once the air-water mixture enters the combustion chamber, the actual heat rate can be determined using the product of the total fluid mass flow rate and the difference in enthalpies of the mixture across the combustion chamber. The temperature at the turbine inlet (state 3) is dependent on the

melting point of the turbine blade material and must be measured or assumed to be a set value. Equation 8 shows the calculation for the heat rate.

$$\dot{Q}_{in} = (\dot{m}_{air} + \dot{m}_{water})(h_{mix,3} - h_{mix,2}) \quad \text{(Equation 8)}$$

After the combustion process, the working fluid passes through the gas generator turbine (GGT). Calculating the enthalpy at the GGT exit requires assuming the power produced by the GGT was equal to the amount required to power the compressor. Using this assumption, the actual enthalpy at state point 4 after the GGT can be calculated and the temperature can be determined. Equations 9 and 10 indicate the relationship between the compressor power and GGT power in terms of enthalpies.

$$\dot{W}_{comp} = \dot{W}_{GGT} \quad \text{(Equation 9)}$$

$$\dot{m}_{air}(h_{air,2} - h_{air,1}) = \dot{m}_{mix}(h_{mix,3} - h_{mix,4}) \quad \text{(Equation 10)}$$

The actual enthalpy, $h_{mix,4}$, can be used to find the temperature at state point 4 after the pressures of each water and air component of the flow have been calculated. Pressure at the GGT exit was calculated using average GGT pressure ratios obtained from experimental data. Entropies can then be determined at the GGT exit in order to calculate the power turbine exit enthalpies at state point 5.

Calculating the enthalpy of the flow after the power turbine (state point 5) requires using the power turbine isentropic efficiency, which is shown in Equation 11 with actual values denoted by an “a” and isentropic values denoted by an “s.”

$$\eta_{PT} = \frac{w_a}{w_s} = \frac{h_{mix,4} - h_{mix,5a}}{h_{mix,4} - h_{mix,5s}} \quad \text{(Equation 11)}$$

Using the isentropic power turbine efficiency and calculated pressures and entropies from the GGT exit, the actual total enthalpy value can be calculated using Equation 11. This total mixture enthalpy is defined in Equation 12 as the sums of the individual air and water components divided by the total mass.

$$h_{mix} = \frac{\dot{m}_{air} \times h_{air} + \dot{m}_{water} \times h_{water}}{\dot{m}_{mix}} \quad \text{(Equation 12)}$$

Using Equation 12, the temperatures and enthalpies of the individual air and water components at the power turbine exit can be calculated with the knowledge that the temperatures of each component are both equal to a single final mixture temperature.

Analysis of the gas turbine cycle involves examining the various power inputs and outputs of the engine. Equations 13-15 show the calculations for compressor power, GGT power, and power turbine output, respectively.

$$\dot{W}_{comp} = \dot{m}_{air}(h_{air,2} - h_{air,1}) \quad \text{(Equation 13)}$$

$$\dot{W}_{GGT} = \dot{m}_{mix}(h_{mix,3} - h_{mix,4}) \quad \text{(Equation 14)}$$

$$\dot{W}_{PT} = \dot{m}_{mix}(h_{mix,4} - h_{mix,5}) \quad \text{(Equation 15)}$$

For the theoretical calculations, the GGT power was assumed to be equal to the compressor power, but in actual applications the GGT power is greater than the compressor power since it must also run the auxiliary needs of the turbine. As such, the net power of the gas turbine is defined as shown in Equation 16.

$$\dot{W}_{net} = \dot{W}_{pt} + \dot{W}_{ggt} - \dot{W}_{comp} \quad \text{(Equation 16)}$$

The net power was used to calculate the indicated horsepower (IHP), which is solely a function of the enthalpies and mass flow rates. During experimental analysis, brake horsepower (BHP) was calculated using measurements of torque and speed from the brake dynamometer attached to the power shaft of the gas turbine. Brake horsepower is related to the indicated horsepower by a mechanical efficiency that accounts for mechanical losses on the shaft and in any reduction gears. In addition to the power metrics, the brake specific fuel consumption (BSFC) is defined as the ratio of the fuel flow rate to the engine power. This ratio is shown in Equation 17. The BSFC indicates how much fuel flow is needed to supply a specific amount of power.

$$BSFC = \frac{\dot{m}_{fuel}}{BHP} \qquad \text{(Equation 17)}$$

Lastly, overall thermal efficiency of the cycle will be calculated as shown previously in Equation 2. An alternative method of calculating the cycle efficiency will also be used during the experimental analysis which incorporates the mechanical inefficiencies inherent to the system. This efficiency, also called the whole engine efficiency, is calculated according to Equation 18.

$$\eta_{engine} = \frac{BHP}{\dot{m}_{fuel} \times LHV_{fuel}} \qquad \text{(Equation 18)}$$

4.3. Discussion

Parametric studies were conducted using the EES program to investigate the effects of post-compressor water injection on horsepower, brake specific fuel consumption, combustor inlet temperature, and efficiency. The effects of changing injection temperature on the aforementioned metrics were also examined. Experimental data from previous runs of the gas turbine were used for the isentropic component efficiencies of the compressor and turbines as

well as the sample data values needed for the theoretical analysis. Due to negligible differences between the results of the competing assumptions regarding the mixing pressure, the analysis was conducted assuming the partial pressure of the air remained constant before and after mixing. The results displayed are for the engine operating at 100% throttle with a fixed combustor temperature.

As Figure 9 indicates, increasing the flow rate of water at 100% throttle increased the brake horsepower if combustor temperature was held constant. Adding water increased the mass flowing through the power turbine and added energy to the airstream, causing an increase in net power from the engine. Heating the water prior to injection did not have an observable effect on the brake horsepower since its effect on the enthalpy of the water was too small to make a significant difference in the power output. In Figure 9, the mass ratio of water to air on the horizontal axis represents increasing the water flow rate for a constant air flow rate.

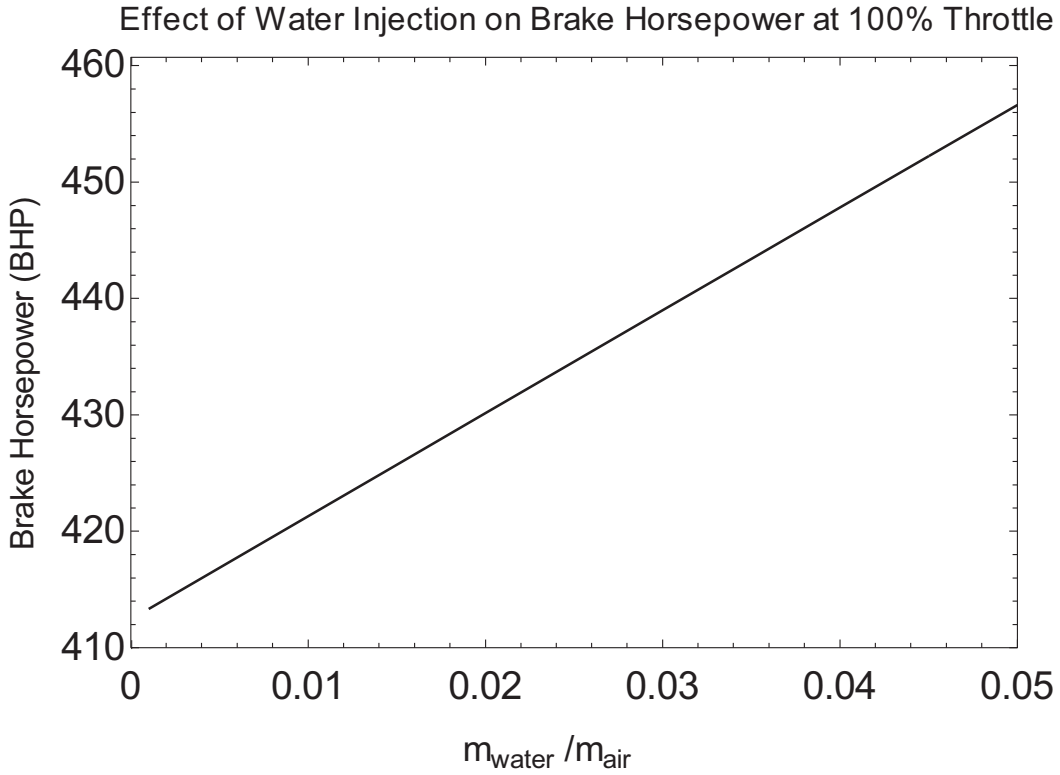

Figure 9: Effect of water injection on brake horsepower

Although water injection increased the power output, it also increased the heat rate into the engine because some of the energy from the combustion reaction was used to vaporize the water. Additional energy must be used to heat the air-water mixture back to the fixed combustor temperature. Figure 10 shows the increase in heat rate as the water flow rate increased. For the analysis, the energy needed to heat the water was assumed to be provided by a waste heat recovery system, so it was not included in the heat rate. Heating the water before injection increased the energy of the water, so the resulting air-water mixture also experienced an increase in energy. Consequently, less fuel energy was needed to heat the air-water mixture up to the designed combustion temperature when the water temperature was increased, causing a marginal decrease in heat rate.

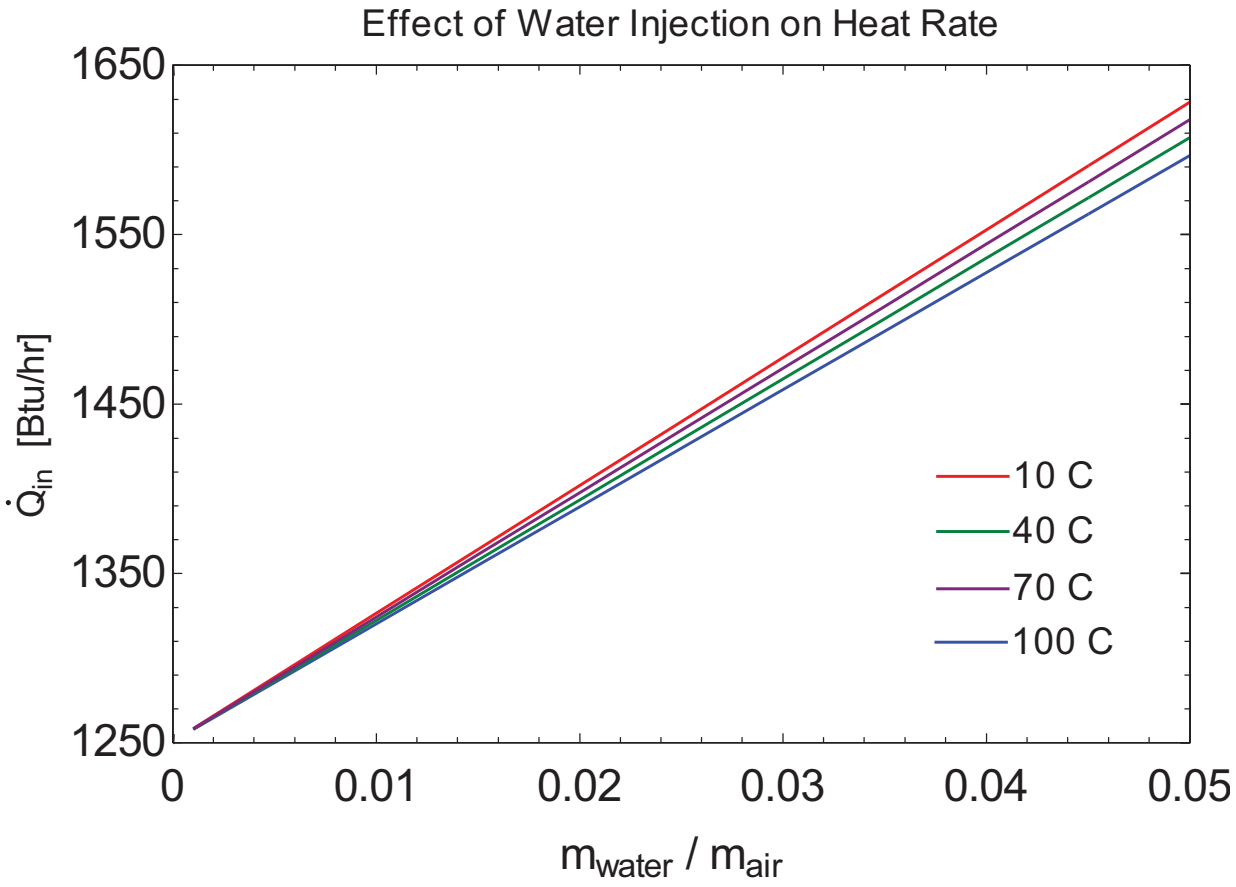

Figure 10: Effect of water injection on heat rate into the combustor

As previously shown in Equation 2, the thermal efficiency is the ratio of the power output to the heat rate. Although the net power output increased as the water mass flow rate increased, the heat rate increased to a greater degree, causing an overall decrease in cycle thermal efficiency. Figure 11 shows the decrease in thermal efficiency caused by increasing the water mass flow rate. Increasing the water temperature slightly increased the thermal efficiency since it decreased the heat rate into the combustor, but the effects were minimal in comparison with the magnitude of the thermal efficiency values.

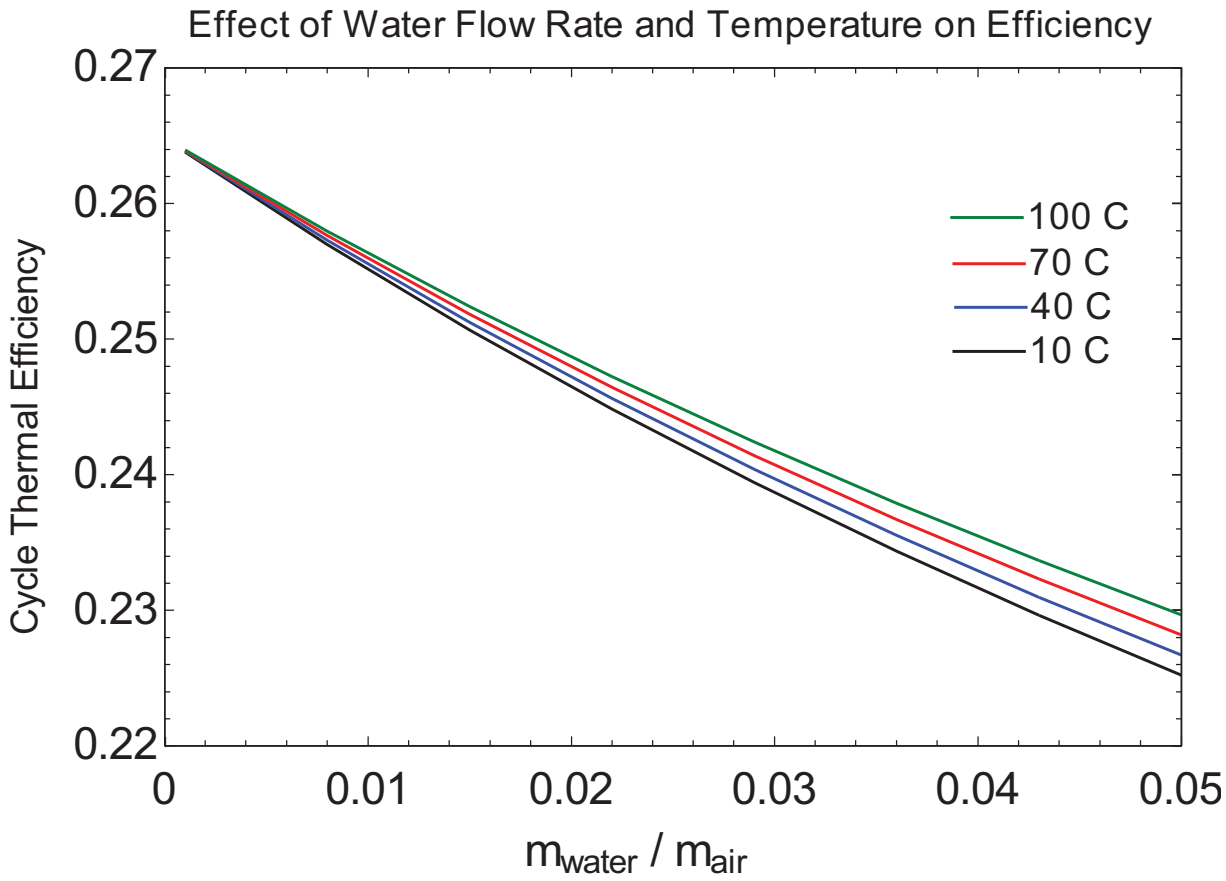

Figure 11: Effects of water injection on thermal efficiency

While heating the water prior to injection showed minimal improvement to the thermal efficiency, its effect on the temperature after mixing could portend significant changes in emissions levels. The temperature after mixing was assumed to be equal to the compressor

discharge temperature, which would in turn affect the combustor temperature. Although the combustor temperature was fixed for the theoretical calculations, the actual combustor temperature would be expected to change as the compressor discharge temperature changed. Combustion temperature controls the level of thermal NO_x emissions, so fluctuations in the mixing temperature would indicate greater variation in the levels of NO_x, carbon monoxide, and unburned hydrocarbons produced by the engine. Figure 12 displays the results of analyzing the compressor discharge temperature with respect to the mass and temperature of the water injected.

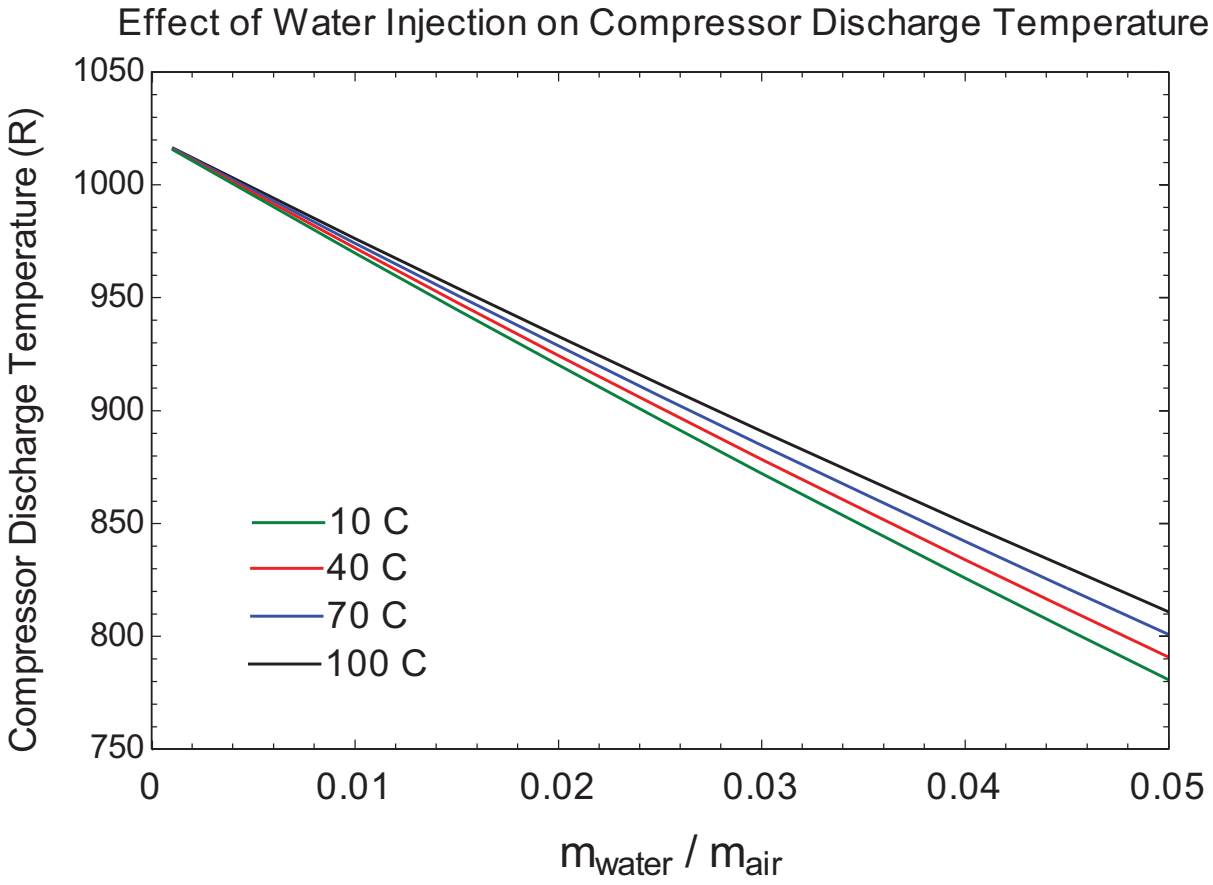

Figure 12: Effect of water injection on compressor discharge temperatures

Increasing the mass flow rate of water decreased the compressor discharge temperatures in the calculations, but increasing the temperature of the water allowed the mixing temperature to be

increased slightly for a specific mass flow rate of water. These trends are expected to also be observed in the experimentally-measured combustor temperatures. Since even small changes in combustor temperature can affect NO_x, CO, and hydrocarbon emissions, combining the effects of changing both the water flow rate and the water temperature on the combustor temperature could yield more insight into the different options that could be available for emissions control using water injection.

5. EXPERIMENTAL METHODOLOGY

5.1. Experimental Test Plan

The test plan for the project consisted of varying the throttle setting of the engine at different mass flow rates of water injected into the compressor discharge airstream. Throttle was varied from 30% to 100% for the baseline runs as well as the tests of seven different water flow rates: 0.1 gpm, 0.3 gpm, 0.4 gpm, 0.5 gpm, 0.6 gpm, 0.7 gpm, and 0.8 gpm. The maximum flow rate of 0.8 gpm was settled on after water mist began flowing from a portion of the gas turbine air tubes that was unsealed to the atmosphere. It was equal to 3.2% of the maximum baseline air flow rate by mass. Tests at higher flow rates were canceled in order to prevent too much water from accumulating in the gas turbines lab. All the flow rate tests were initially conducted with tap water at its delivery temperature of 15ºC. Additional tests were later conducted for the 0.4 gpm and 0.6 gpm flow scenarios in which the water temperature was changed to 45ºC and 60ºC. The maximum temperature of 60°C was chosen based on the most consistent temperature that was achieved by adjusting the water heater thermostats to their hottest settings.

For all the spray tests, throttle was increased from the idling setting at 30% up to 100% throttle and then decreased back down to 30% before the engine was shut off. Throttle was

increased from 30% to 70% by 20% increments, from 70% to 80% by 5% increments, and from 80% to 100% by 2% increments. The throttle settings were adjusted in the same manner in reverse as throttle was decreased back to 30% from 100%. Table 1 displays the experimental test matrix that guided the data collection. All data runs shown in Table 1 were successfully conducted on the Rolls-Royce Model 250.

Table 1: Experimental test matrix

Throttle (%)	Spray Tests: Flow rate (gpm), Water Temperature (ºC)										
	0.1, 15C	0.3, 15C	0.4, 15C	0.5, 15C	0.6, 15C	0.7, 15C	0.8, 15C	0.4, 45C	0.4, 60C	0.6, 45C	0.6, 60C
30											
50											
70											
75											
80											
82											
84											
86											
88											
90											
92											
94											
96											
98											
100											

5.2. Spray System Fabrication and Assembly

In order to deliver the water to the compressor discharge airstream, an original spray system was constructed that could control the temperature and volumetric flow rate of water into the engine while ensuring the smallest possible droplet sizes for optimal vaporization inside the turbine. The spray system was designed to generate at least enough pressure to overcome the compressor discharge pressure while delivering the water at the desired flow rates. A schematic of the spray system is shown in Figure 13.

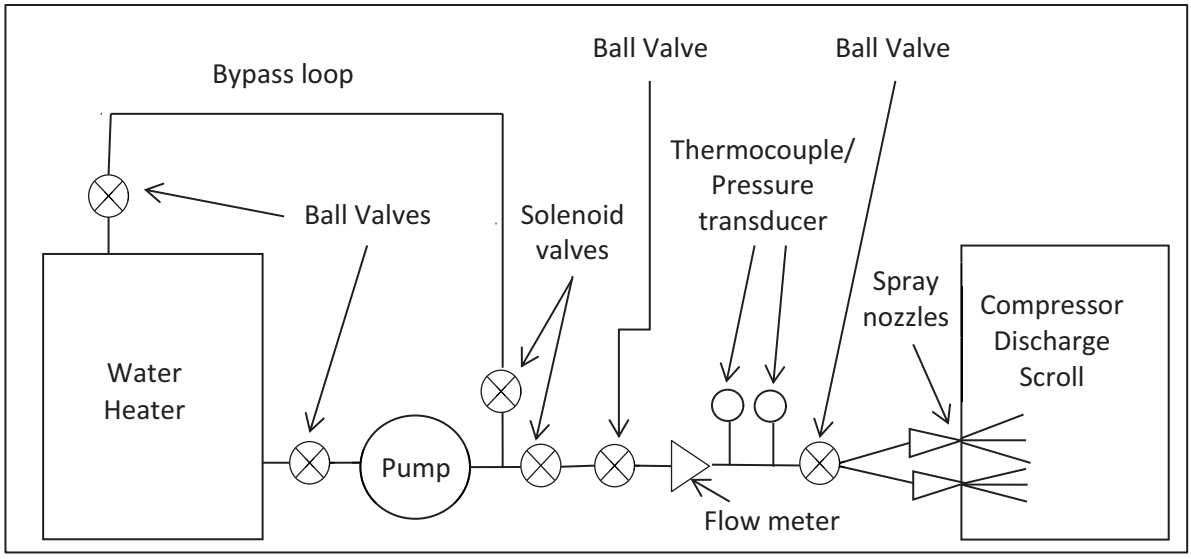

Figure 13: Spray system configuration schematic

The first component was a commercial 35 gallon water heater stored in the Rickover Gas Turbines Lab. It was used to both store and heat the water using thermostats that could be operated between 110ºF and 160ºF when energized. A ball valve was installed downstream of the water heater in order to regulate water flow from the tank to the rest of the spray system. In order to generate the flow rates and pressure needed to inject water into the compressor discharge airstream, a hydraulic gear pump capable of producing 1.6 gpm of flow at pressures up to 1000 psi was installed downstream of the ball valve. It was mounted to a ½ hp variable-speed DC motor. An image of the pump and motor assembly is shown in Figure 14.

Figure 14: Pump and motor mounting assembly

During the data collection runs, the desired flow rates were set using the variable speed controller on the motor. For safety reasons, operation of the gas turbine had to be observed from the control room overlooking the laboratory, so the pump needed to be energized and running at the desired speed before the engine could be started. To avoid spraying into the turbine before the engine was started, a solenoid-controlled bypass system was installed directly downstream of the pump. A normally-closed solenoid valve was used to prevent flow from reaching the nozzles unless energized. This valve diverted the water into a bypass loop that fed back to the water heater. The bypass loop was implemented to prevent a large pressure build-up at the pump discharge due to the accumulation of flow. Excessive pump discharge pressures posed the risk of damaging the pump.

A second solenoid valve, normally open, was installed on the bypass loop itself to close off flow to the water heater when energized. Both the normally-open and normally-closed solenoid valves were wired to the same outlet strip in the control room so one would close and the other would open at the same time. Through this configuration, when both solenoids were de-energized, the pump could be dialed to the desired speed and would pump water back to the water heater through the bypass loop until it was time to begin spraying. At that time, energizing the solenoids would simultaneously close off the bypass loop and open the spray line to the nozzles, allowing water to enter the engine. Additionally, since the two solenoid valves were designed for maximum pressure differentials of 250 psi and 300 psi, a mechanical pressure gauge was installed within the bypass loop so the spray line pressure could be monitored during spray system testing and calibration. An image of the bypass part of the spray system is displayed in Figure 15.

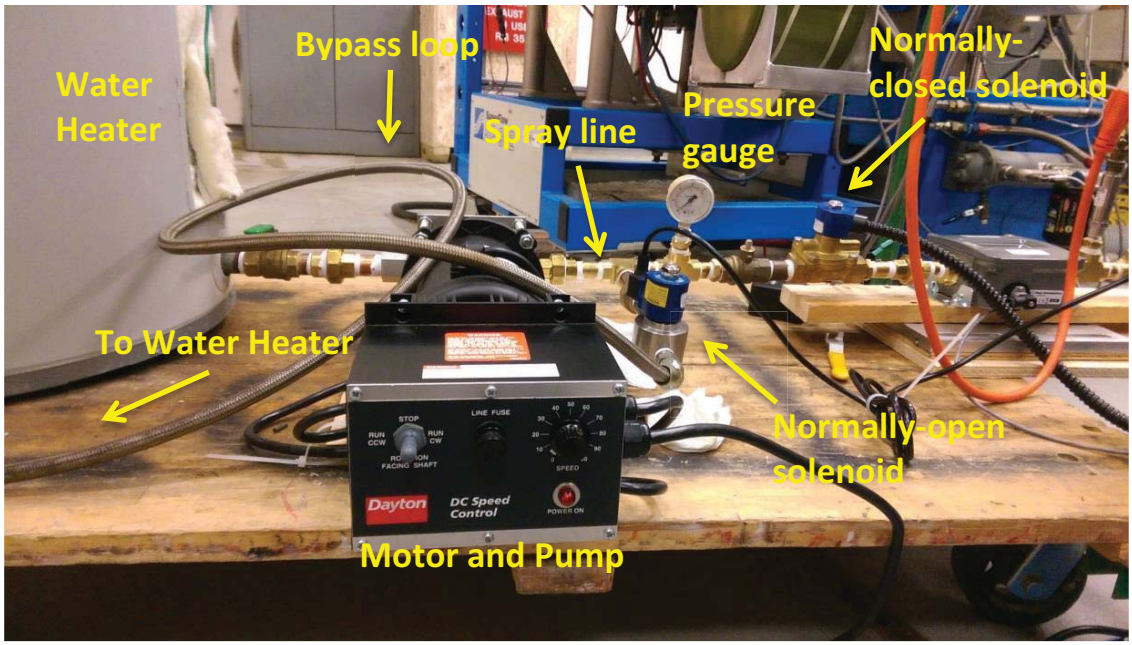

Figure 15: Bypass loop system side view

Downstream of the normally-closed solenoid, the water flow rate was measured using an Omega® MR Flow transmitter, a variable area flow meter capable of reading flow rates between 0.2 gpm and 2.0 gpm. Pressure and temperature of the water were measured directly downstream of the flow meter using an Omega® piezoresistive pressure transducer and a thermocouple. From the thermocouple, the water was sent through a braided steel hose to the compressor discharge. Figure 16 illustrates the part of the spray system downstream of the bypass loop.

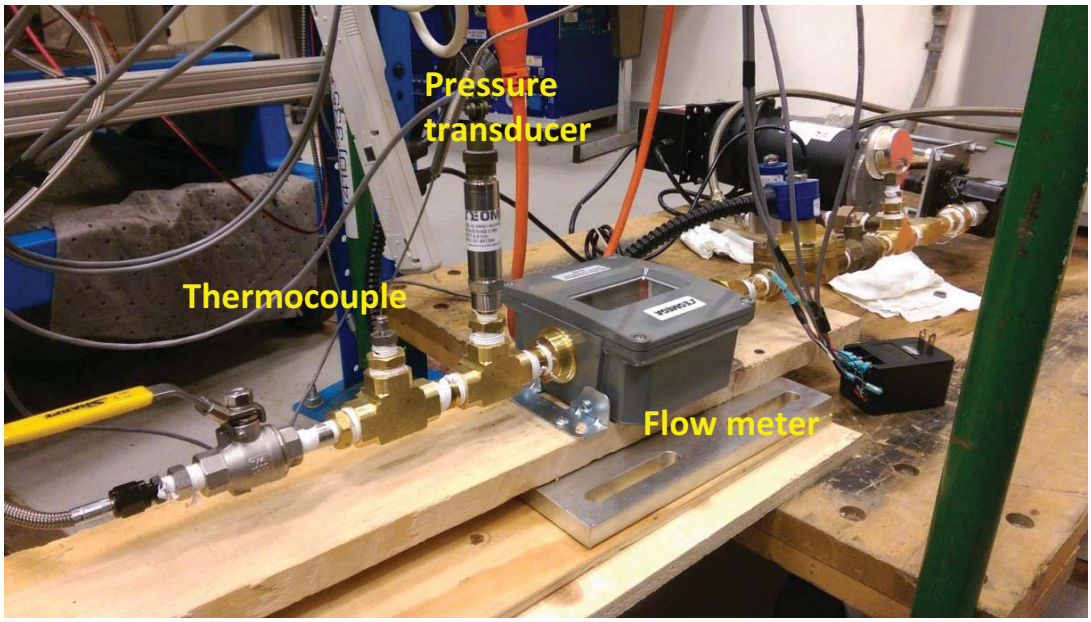

Figure 16: Downstream spray assembly

Once the water reached the braided steel hose, it was split in two and injected at two locations into the compressor discharge scroll. The flow was split in order to distribute the water spray more evenly between the two air tubes leading to the combustion chamber. A photograph of the injection sites is shown in Figure 17.

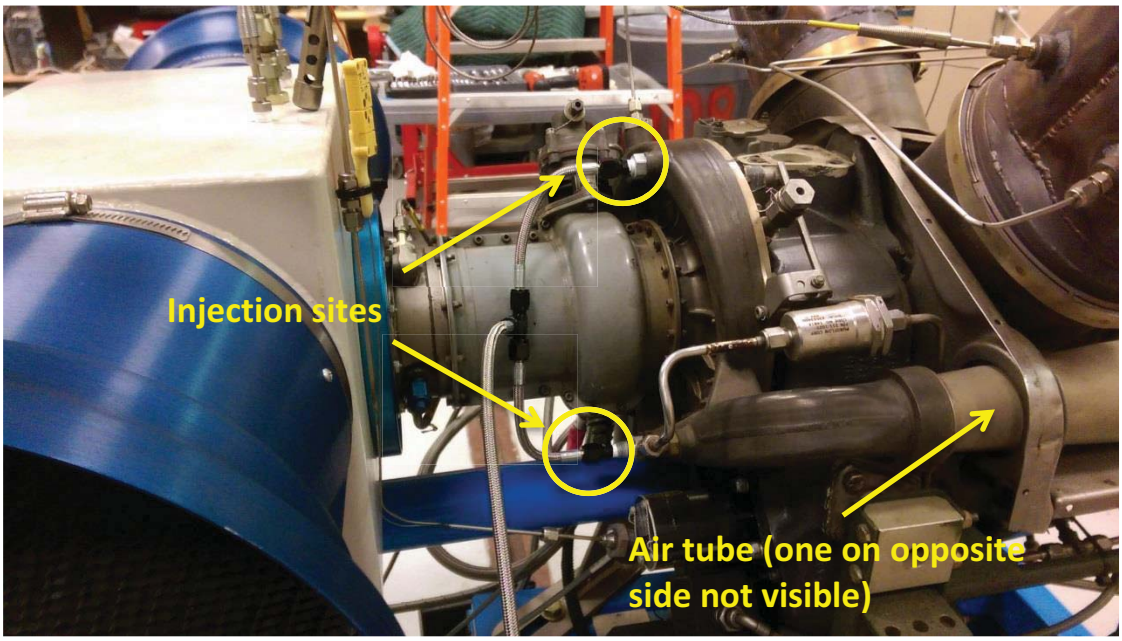

Figure 17: Injection sites

At the compressor discharge scroll, special fittings fabricated with the help of the Naval

Academy's Machine Shop were used to install the spray nozzles into the engine. The nozzles were installed in ports at the compressor discharge scroll that were either unused or being used for supplementary Kiel probes. Existing plugs for these ports were removed and replaced with the specially fabricated fittings with the nozzles attached. Figure 18 shows the nozzle fittings with the nozzles installed in them.

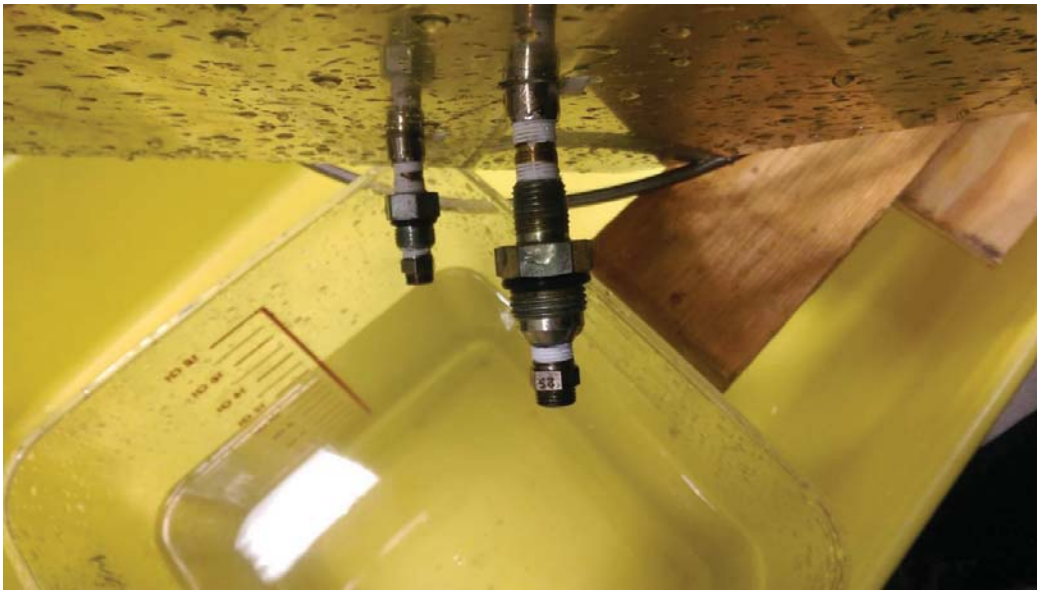

Figure 18: Nozzle fittings

Fog droplet studies conducted by Mustapha Chaker, Cyrus Meher-Homji, and Thomas Mee indicated that smaller droplets, between 5 to 15 microns in diameter, were advantageous for inlet fogging applications [14]. This range was determined based on experiments that showed that droplets of these sizes were more likely to remain entrained in the air flow and did not show erosion effects on the compressor blades. The optimal droplet diameter range for inlet fogging applications was also assumed to be applicable to post-compression water injection systems, which involve evaporation in a higher pressure and temperature air stream than that of inlet fogging. However, the back pressures needed to achieve such small droplet diameters were in the 2000-3000 psig range and were thus impractical given the available equipment.

Various nozzles and manufacturers were evaluated, but ultimately ease of installation

directed the choice of nozzle toward nozzles used for water and methanol injection in automobiles. Nozzles with different sized orifices needed to be used to cover the full range of flow rates, so nozzles with four different flow rate capacities were used based on the manufacturer's published data at 200 psi back pressure: 3.00 gph, 8.00 gph, 16.00 gph, and 25 gph. Each of the nozzles had 1/8"-27 National Pipe Thread (NPT) Taper connections with a 7/16" wrench hexagonal flat for ease of installation and removal. Based on manufacturer claims, these nozzles were capable of delivering spray with droplet diameters in the range of 50-70 μm. These droplet sizes corresponded to typical droplet sizes for water spray applications in automobiles. The nozzles were capable of delivering water at the desired flow rates and pressures and are shown in Figure 19.

Figure 19: Spray Nozzles (3.00 gph nozzles not shown)

The result of the fabrication and assembly process was a spray system that could be controlled using the variable speed motor to produce flow rates between 0 and approximately 1.2 gpm, depending on the size of nozzle used. Additionally, the system allowed the user to activate and deactivate the water spray while monitoring the operating conditions remotely from the control

room. The finished system could be left running without damaging the pump or spraying water into the engine until the desired throttle condition was met for water spray. At that time, the spray system would deliver a consistent flow rate at back pressures great enough to overcome the pressure inside the compressor discharge. Figure 20 displays the completed spray system.

Figure 20: Finished spray assembly

5.3. Engine Instrumentation and Data Acquisition Process

Data were acquired to characterize the effects of post-compression water injection on the Rolls-Royce M250. The instrumentation needed for data collection was installed on the engine in 2007 using the SuperFlow™ Computerized engine test system. Thermocouples and pressure transducers were placed at each of the major thermodynamic state points of the engine while flow meters were used at various locations on the engine to measure air and fuel flow. Torque and power were calculated using a dynamometer fixed to the power turbine output shaft. Signals from these instruments were collected and interpreted by the WinDyn computer program, which is the data acquisition system for the SuperFlow™ console. The instrumentation had been calibrated in the WinDyn system upon installation.

In addition to the existing instrumentation, an Infrared Industries Five Gas Analyzer was installed on the gas turbine to collect emissions data. The Five Gas Analyzer used was recently purchased in 2014 and had been calibrated by the manufacturer. Figure 21 shows the Five Gas Analyzer used for the tests along with the location from which it drew the exhaust gases on the exhaust pipe. A rubber hose connected a gas input at the back of the analyzer with the exhaust probe.

Figure 21: Five Gas Analyzer with exhaust port location

Figure 22 shows a schematic of the engine setup with key instrumentation locations identified. The schematic also shows how the SuperFlow^{TM} consoles were incorporated into the system.

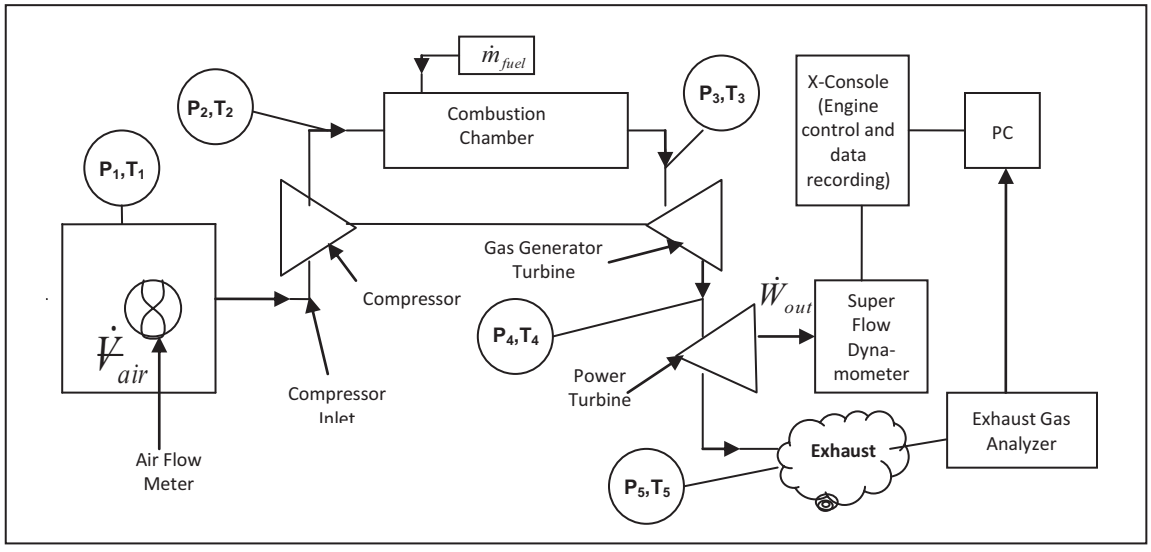

Figure 22: Schematic of engine with instrumentation points

Separate from the engine instrumentation, a flow meter, thermocouple, and pressure transducer were added to the spray assembly to monitor and control the water spray. The flow

meter and pressure transducer were wired from the gas turbines laboratory directly upstairs to a multimeter inside the control room. Their voltage readings were used to calculate the measured flowrates and pressures. Multimeter calibration tests were conducted and verified with published manufacturer's data. Figure 23 shows the SuperFlow™ engine control console located in the gas turbines control room along with the multimeter used to record output voltage from the flow meter and pressure transducer.

Figure 23: SuperFlow™ control console with multimeter

5.4. Procedures

Before conducting spray tests using the spray assembly, the motor speed settings needed to be calibrated to the desired nozzle flow rates. The spray system was tested by pumping the water into a graduated bucket at atmospheric pressure. For flow rates greater than 0.2 gpm, the motor was adjusted until the flow meter display read the desired flow rate. Calibration of the motor to flow rates below 0.2 gpm required the use of a scale and a stopwatch in order to determine the mass of water that was discharged into the bucket over one minute. The motor speeds that corresponded to each desired flow rate were used to determine the target back pressures within the spray line needed to maintain the same flow rate once the spray was injected

into the compressor discharge.

Using the known compressor discharge pressure, target back pressures were calculated using Bernoulli's principle for an incompressible liquid. The calculations determined that the compressor discharge pressure needed to be added to the pressure obtained from spraying into the atmosphere in order to get the target back pressure needed to maintain the same flow rate spraying into the compressor discharge. The motor speeds needed to generate the new target pressures when spraying into the atmosphere were then determined through further spray system calibration. Once testing began, fine-tuning of the motor speeds was conducted to ensure the correct water flow rates were being generated once the spray was entering the compressor discharge. Table 2 shows the final motor speed settings needed to produce all the flow rates tested, along with the rated capacity of the nozzle used for each flow rate.

Table 2: Final motor speed flow rate calibrations

Flow Rate (gpm)	Nozzle Capacity	Motor speed setting (%)
0.1	3.00 gph	24
0.3	8.00 gph	32
0.4	8.00 gph	40
0.5	8.00 gph	39
0.6	16.00 gph	45
0.7	16.00 gph	52
0.8	25.00 gph	55

During engine operation, the motor would be energized and set to the desired speed before the gas turbines laboratory was vacated. From the control room, the engine was ignited and allowed to idle before the data collection runs began. The standard operating procedures for the Rolls-Royce Model 250 are included as Appendix B. The gas analyzer took approximately 15 seconds to accurately read the exhaust gas composition, so at least that amount of time was spent at each throttle setting. At 80% throttle, the spray system was activated and was not deactivated until 80% throttle was passed on the way back down from 100% throttle. The choice

of 80% throttle as the spray start and finish was based on the throttle setting at which the power turbine reached its designed rotational speed based on a fixed dynamometer speed of 6000 rpm. This rotational speed was the turboshaft speed of the helicopter engines that the Rolls-Royce M250 powered. For engine throttle levels below 80%, the dynamometer continued to increase in speed as the output shaft speed increased. Above 80% throttle, the dynamometer was fixed at 6000 rpm. After each run, the gas turbine was shut off and the gas analyzers were reset in order to re-zero the measurements.

6. RESULTS

6.1. Baseline Data Reduction and Results

An understanding of the Model 250's operating characteristics under normal operating conditions was necessary to evaluate the effects of post-compression water injection on its performance and emissions. Ten different baseline, no-spray tests were conducted over several weeks to verify repeatability. Operation of the engine followed the steps outlined in the procedures. Performance metrics such as corrected power, brake specific fuel consumption, and GGT speed were compared with each other to investigate turbine performance and operating characteristics without water injection. Figure 24 demonstrates the relationship between throttle setting and power output corrected to the standard atmospheric conditions used by the gas turbines industry (14.67 psia and 60ºF).

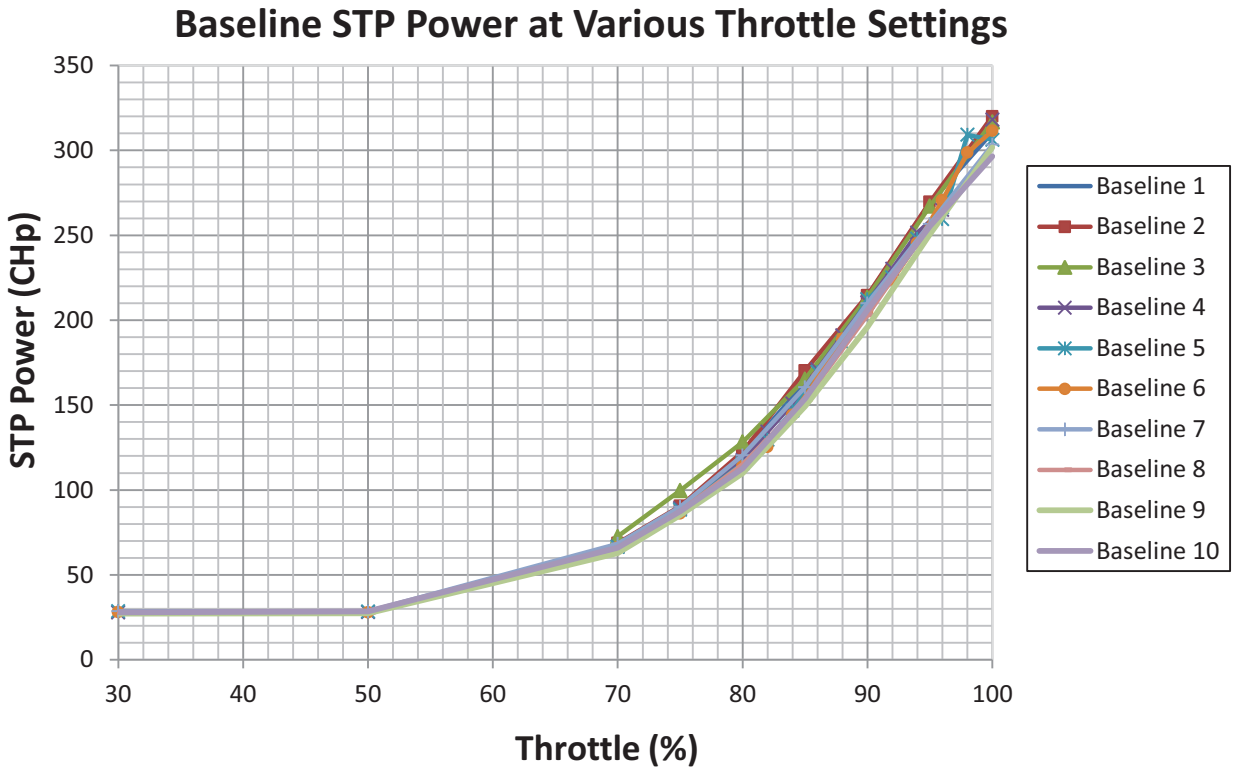

Figure 24: Baseline STP power at various throttle

As the engine throttle setting was increased, the power calculated from the torque and speed of the water brake dynamometer increased as well. This occurred because increasing the engine's throttle setting increased the flow rate of fuel entering the combustor. Higher fuel flow rates increased the temperature of the products in the combustor and the enthalpy of the gases exiting the combustion chamber. The flow of the higher enthalpy gases through the GGT caused its speed of rotation to increase. Figure 25 shows the increase in GGT speed caused by increasing the throttle setting.

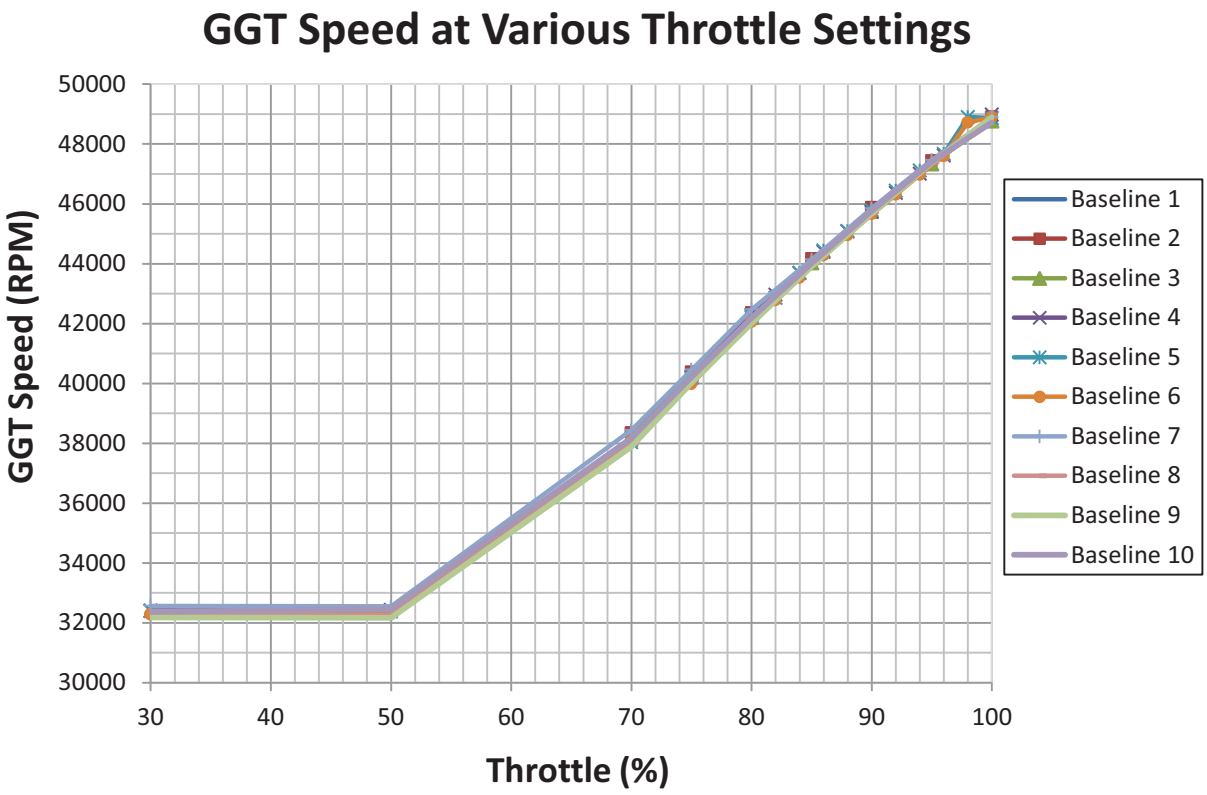

Figure 25: Baseline GGT Speed at various throttle settings

Since the gas generator turbine and compressor were mechanically linked, increasing the GGT speed increased the compressor speed, which in turn increased the compressor work on the inlet air. This increase in compressor work was manifested as an increase in the air mass flow rate and compressor pressure ratio, leading to an increase in the compressor discharge pressure as well.

The increase in compressor work came at the cost of greater energy consumption, so the engine consumed more fuel as the compressor discharge pressure increased. Fuel was regulated through a power turbine fuel governor and GGT fuel control system that scheduled more fuel to the engine as the compressor discharge pressure increased. This fuel control system allowed the engine to support higher GGT speeds at higher throttle levels. At these increased GGT speeds, the increase in air mass flow rate and combustion gas enthalpy allowed the gases at the gas generator turbine exit to have greater enthalpy than at lower throttle settings.

This increase in enthalpy and air flow rate at the GGT exit caused the power turbine to attempt to spin faster as the gases flowed through it. However, since the dynamometer coupled to the output shaft was designed to be fixed at 6000 rpm, the water brake applied more force to hold the dynamometer speed constant. This increase in dynamometer force translated to an increase in the calculated power output of the engine. As a result, as indicated in Figure 26, the power output of the engine increased as the GGT speed increased.

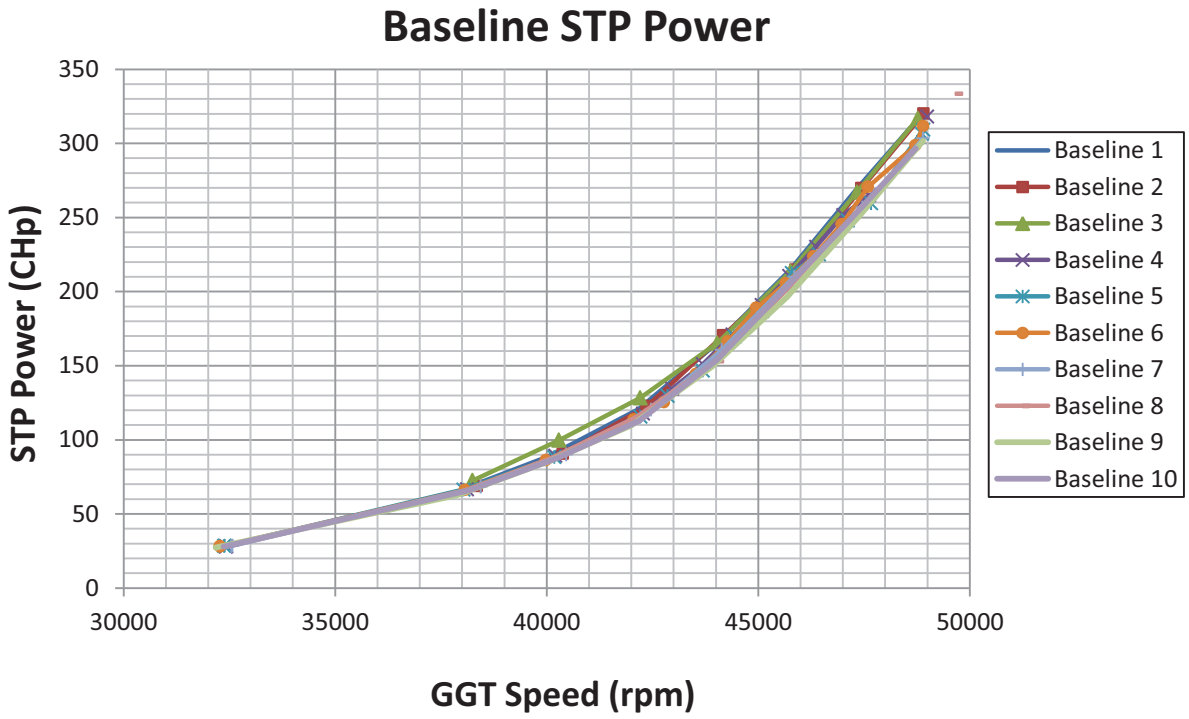

Figure 26: Baseline STP Power at Various GGT Speeds

The increased GGT speed allowed the air mass flow rate through the engine to increase correspondingly, so the power output of the engine also increased as air mass flow rate increased. Figure 27 indicates the relationship between corrected power and the corrected air mass flow rate, a gas turbine industry standard.

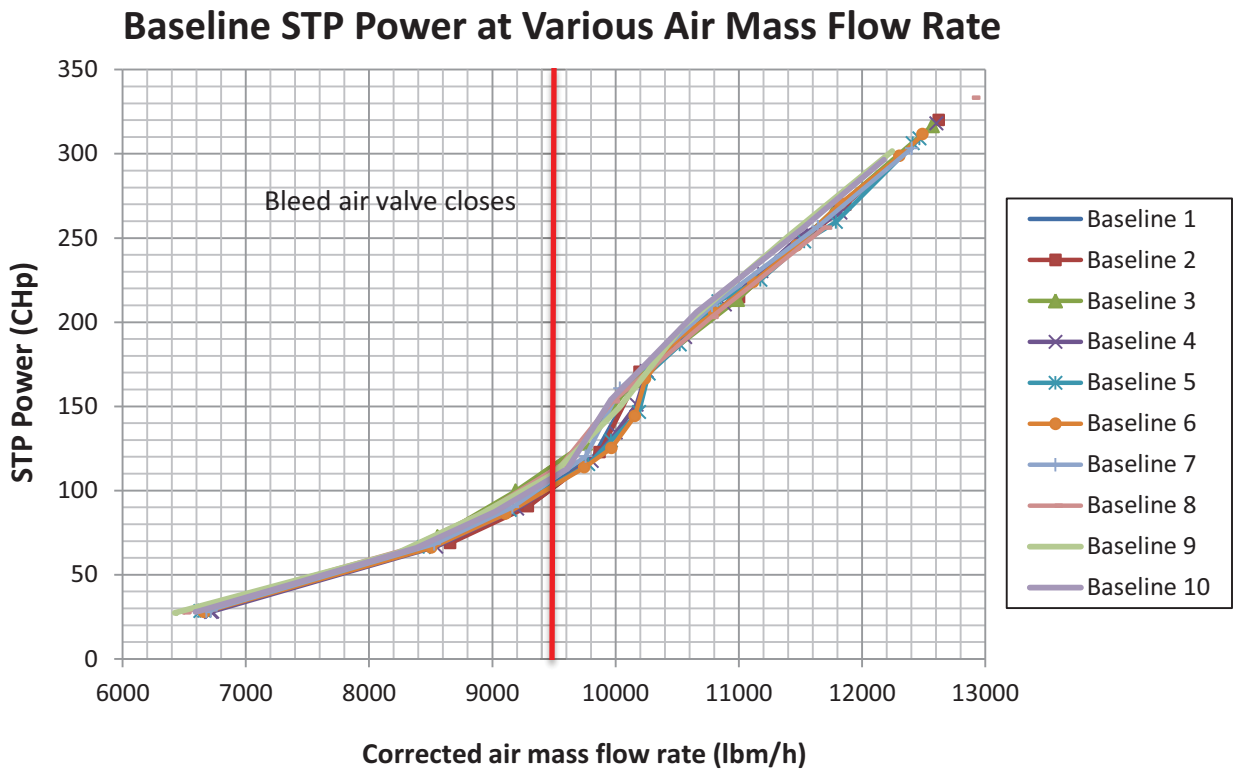

Figure 27: Relationship between STP Power and corrected air mass flow rate

Although the engine power increased in a smooth, exponential fashion as the GGT speed increased, the power output displayed a very noticeable jump in magnitude as the air mass flow rate increased. This jump represents the closing of the start derichment valve, or bleed air valve, as the throttle increased. Up until around 75% throttle, the engine vented some of its internal air flow back to the atmosphere in order to minimize the amount of fuel needed for engine start-up. Once the bleed air valve closed, all the air was diverted through the GGT, allowing the engine to schedule more fuel for acceleration. As a result, the power output increased markedly after the bleed air valve closed.

Variations in the ten baseline runs can be attributed to ambient atmospheric fluctuations across the range of dates that the data were collected. Changes in environmental pressure, temperature, and humidity affected the air density, which in turn affected the amount of work the compressor had to perform during engine operation. As shown in Equation 1, increasing density

decreases compression work while decreasing density causes the work to increase. Atmospheric conditions affected the subsequent spray tests as well as the baseline runs. Even though averages for each spray test were used to evaluate the effects of post-compression water injection compared to the baseline operating condition, the effects of environmental conditions on the perceived results must be accounted for when determining trends in the spray results.

6.2. Spray Results

6.2.1. Effects of Varying Water Flow Rate on Engine Performance and Emissions

In order to evaluate the effects of post-compression water injection on the operating characteristics of the Rolls-Royce M250, the relationships between air and fuel mass flow rates needed to be examined at various water spray flow rates. Figure 28 shows how the air mass flow rate changed for different water spray flow rates as throttle was increased. For all subsequent plots, the baseline results included with the spray results represented the average of all ten runs for each engine characteristic examined.

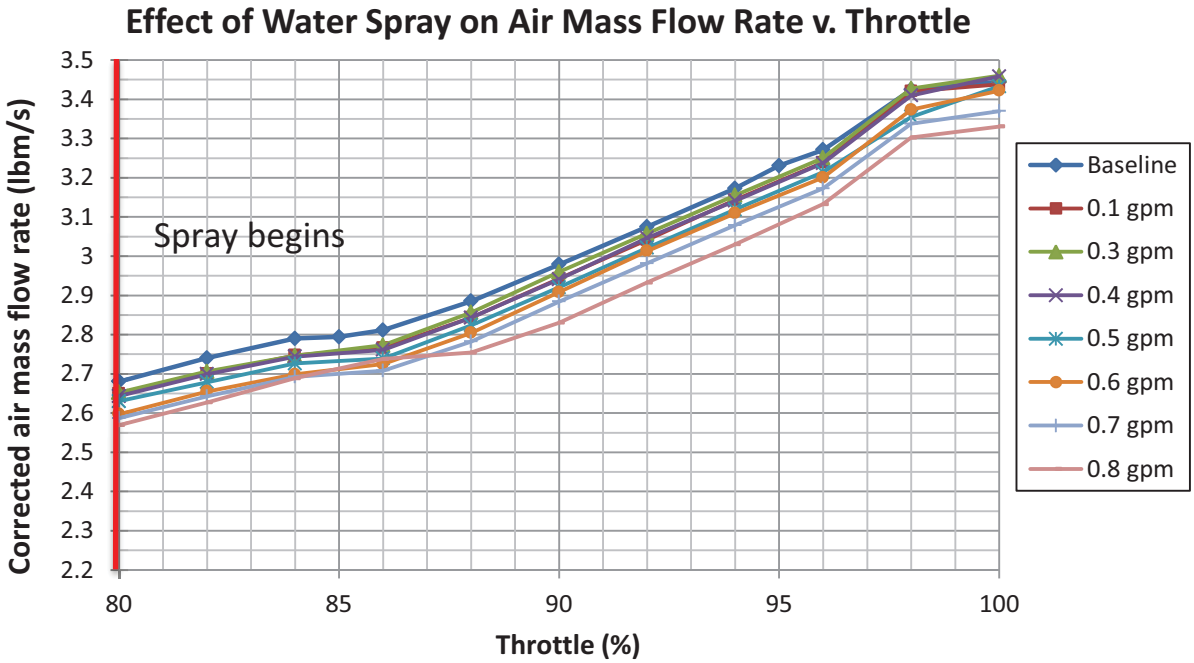

Figure 28: Air mass flow rate at various throttle settings for different spray tests

As Figure 28 indicates, the air mass flow rate decreased for a specific throttle setting as the spray flow rate increased. The reduction in air mass flow rate at each throttle setting caused by the water spray can be explained through examination of the GGT speed at the same throttle settings. Figure 29 shows the GGT speed at different throttle settings after the spray was activated.

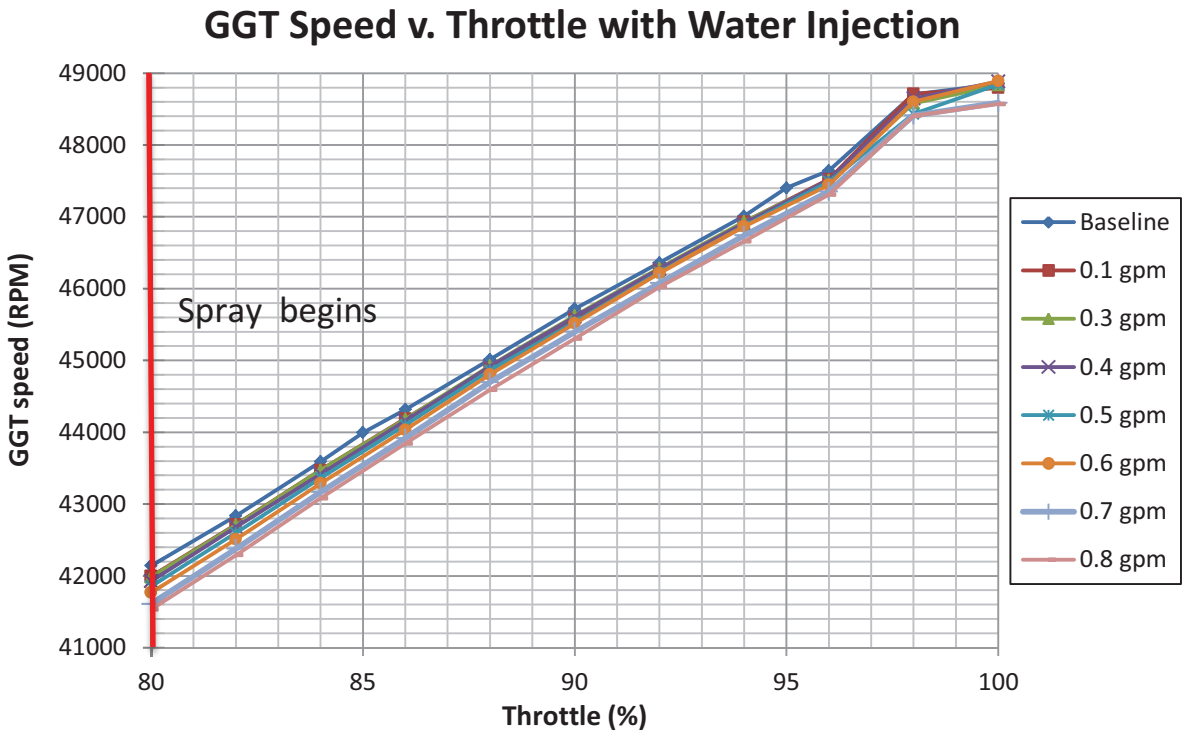

Figure 29: GGT speed v. Throttle for various water flow rates

As throttle increased, the GGT speed at a specific setting decreased as the water flow rate increased. Since the GGT controls the compressor speed, a decrease in GGT speed corresponded to a decrease in compressor speed. At lower speeds of rotation, less air was ingested by the compressor since there was a direct correlation between volumetric flow through the compressor and compressor speed. Figure 30 demonstrates this relationship between GGT speed and the volumetric flow rate of air through the engine.

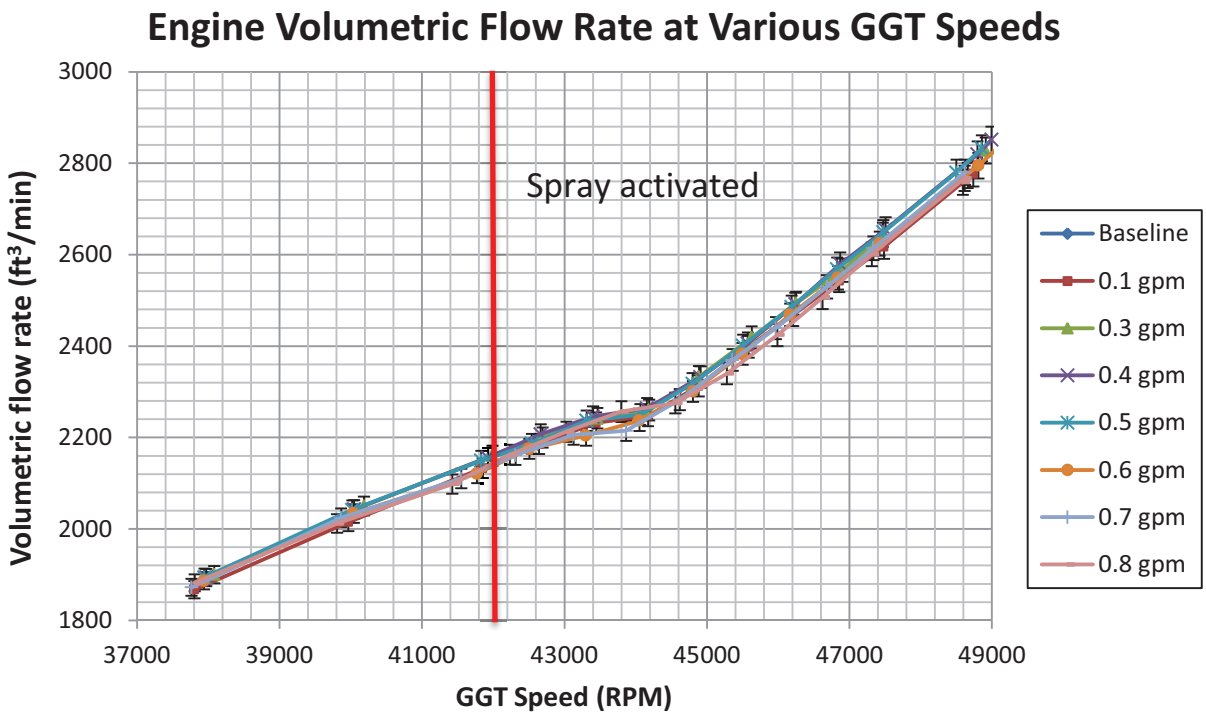

Figure 30: Relationship between flow rate and GGT speed

As Figure 30 indicates, the relationship between volumetric flow rate and GGT speed appeared to be unaffected by changes in water spray flow rate. Variations in volumetric flow rates at the different GGT speeds could be attributed to measurement uncertainty, since all the volumetric flow values ostensibly fell within one percent of each other, as indicated by the error bars included on the figure. This observation corroborated expectations because the volumetric flow rate was solely a function of the compressor design and rotational speed and should not have changed as water was injected into the engine. Increasing the spray flow rate reduced the GGT speed at a specific throttle setting, so the volumetric flow rates corresponding to those GGT speeds also decreased. Since the volumetric flow rates decreased for a specific throttle setting as water was injected, the air mass flow rates also decreased as previously shown in Figure 28. Fluctuations in the air mass flow rate due to atmospheric changes did not appear to affect the general trend that the data displayed.

At the same time that the air mass flow rate decreased, the fuel flow rate increased. Figure 31 shows the effect of spraying water on the fuel consumption of the engine at various GGT speeds. The data are shown starting with the GGT speeds that corresponded to 80% throttle, the start of the water spray.

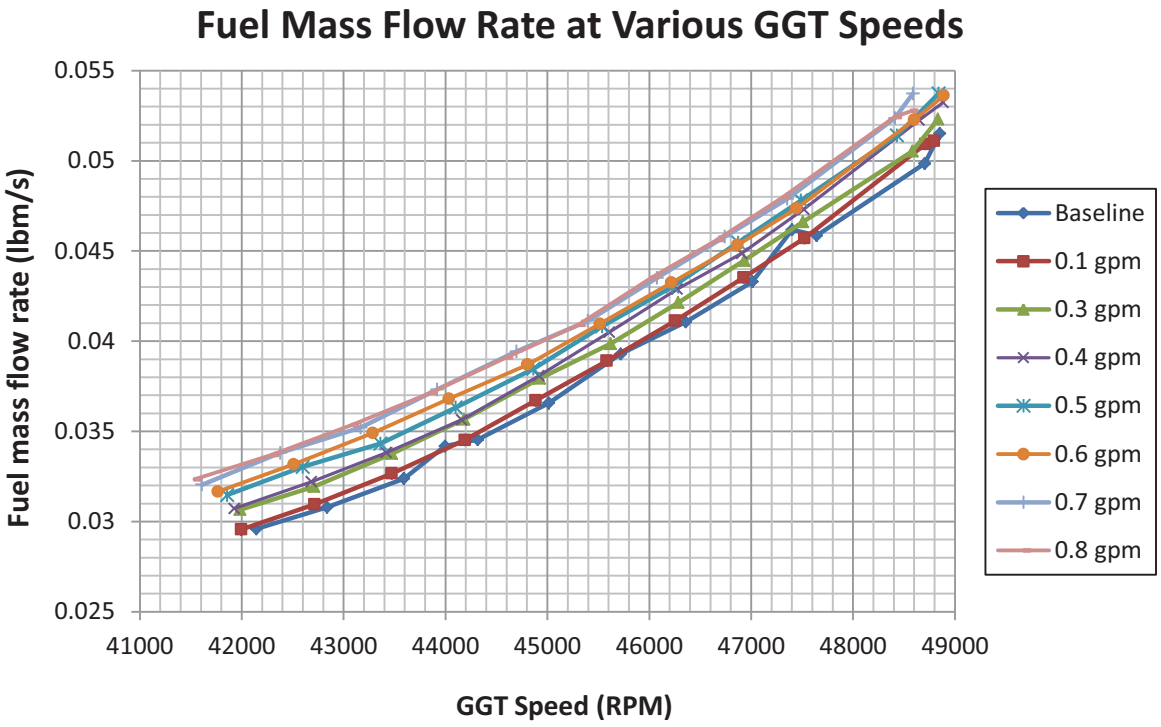

Figure 31: Fuel consumption at various GGT speeds and water spray rates

For a specific GGT operating speed, more fuel was needed to keep the GGT operating at a constant speed as the amount of water injected increased. Since the air mass flow rate decreased for a specific throttle setting and the fuel mass flow rate increased with GGT speed, examining the fuel mass flow rate in comparison with the air mass flow rate showed that the amount of fuel used by the engine at a specific air flow rate increased as the water spray flow rate increased. Consequently, the air-fuel ratio also decreased as the throttle setting increased. Figure 32 shows the relationship between fuel flow rate and air flow rate at specific corrected air flow rates while Figure 33 shows the air-fuel ratios at various throttle settings and water spray flow rates. In

Figure 32, the data are shown starting with the air mass flow rate corresponding to 80% throttle.

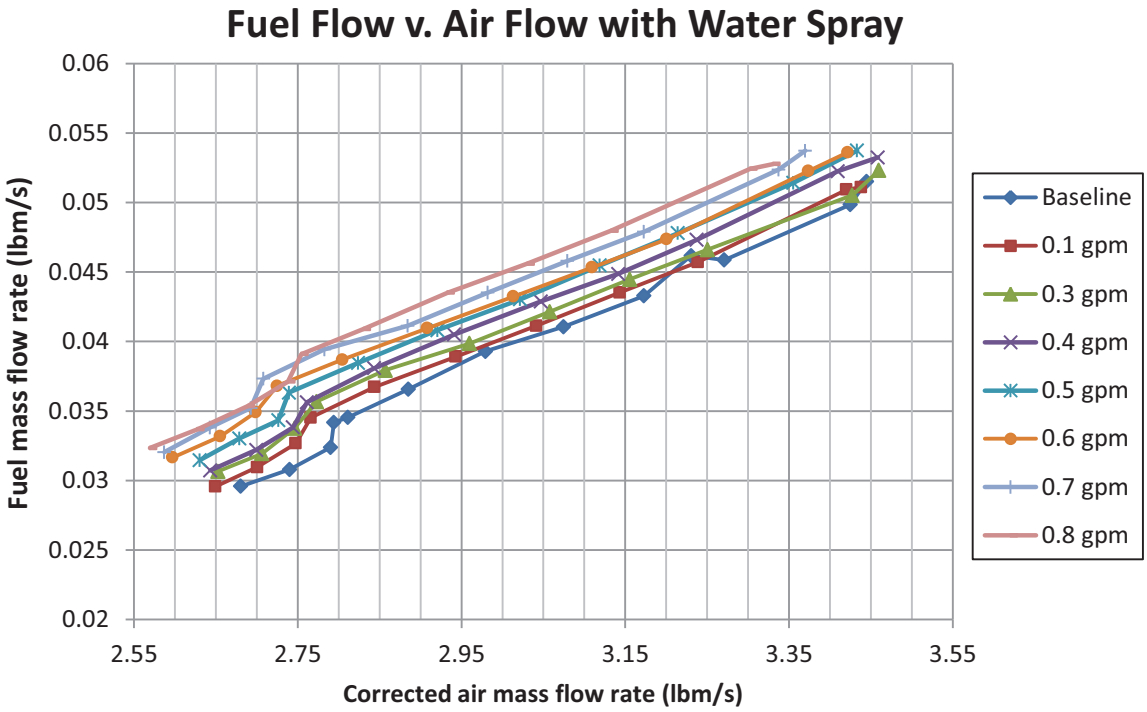

Figure 32: Effect of water spray on Fuel flow rate v. Air flow rate

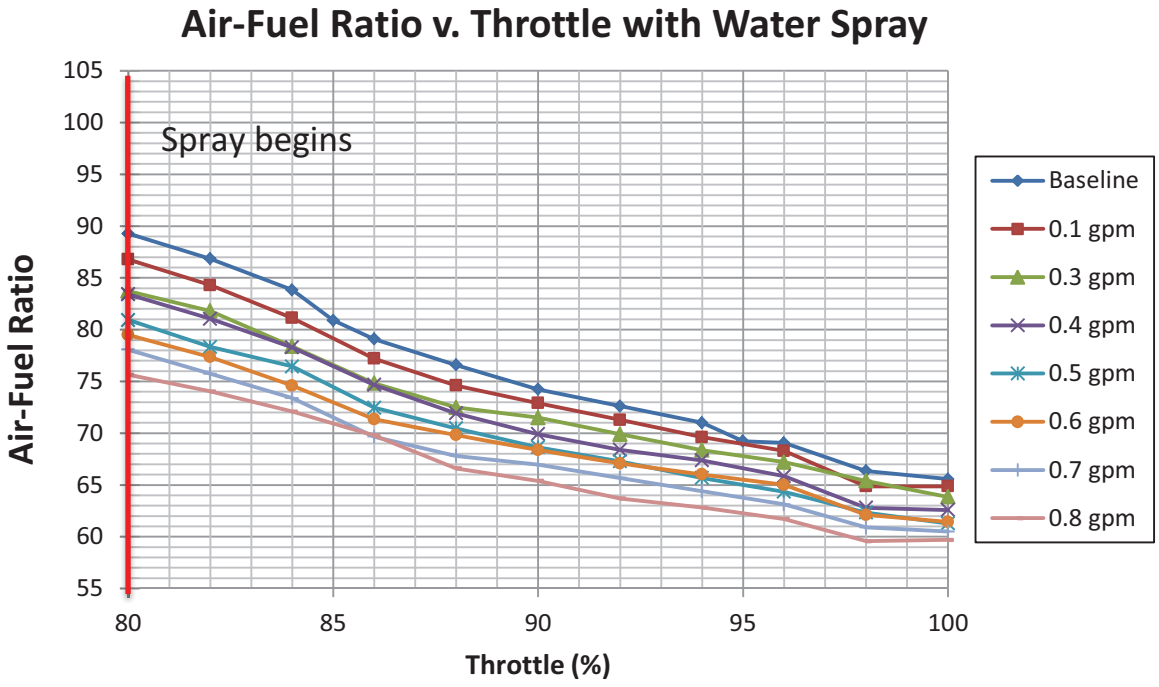

Figure 33: Effect of water spray on Air-fuel ratio v. Throttle

The increase in fuel flow observed from increasing the water spray may be attributed to a

decrease in combustor temperature that occurred when water was injected into the gas turbine cycle. Some of the energy from burning the fuel in the combustor was absorbed into both the sensible heating of the added water mass and the latent heat of vaporization of the water droplets. As a result, the flame temperature decreased. Figure 34 shows the decrease in combustor temperature at various GGT speeds for different water spray flow rates. The data are displayed starting with the values for GGT speed when the spray began at 80% throttle.

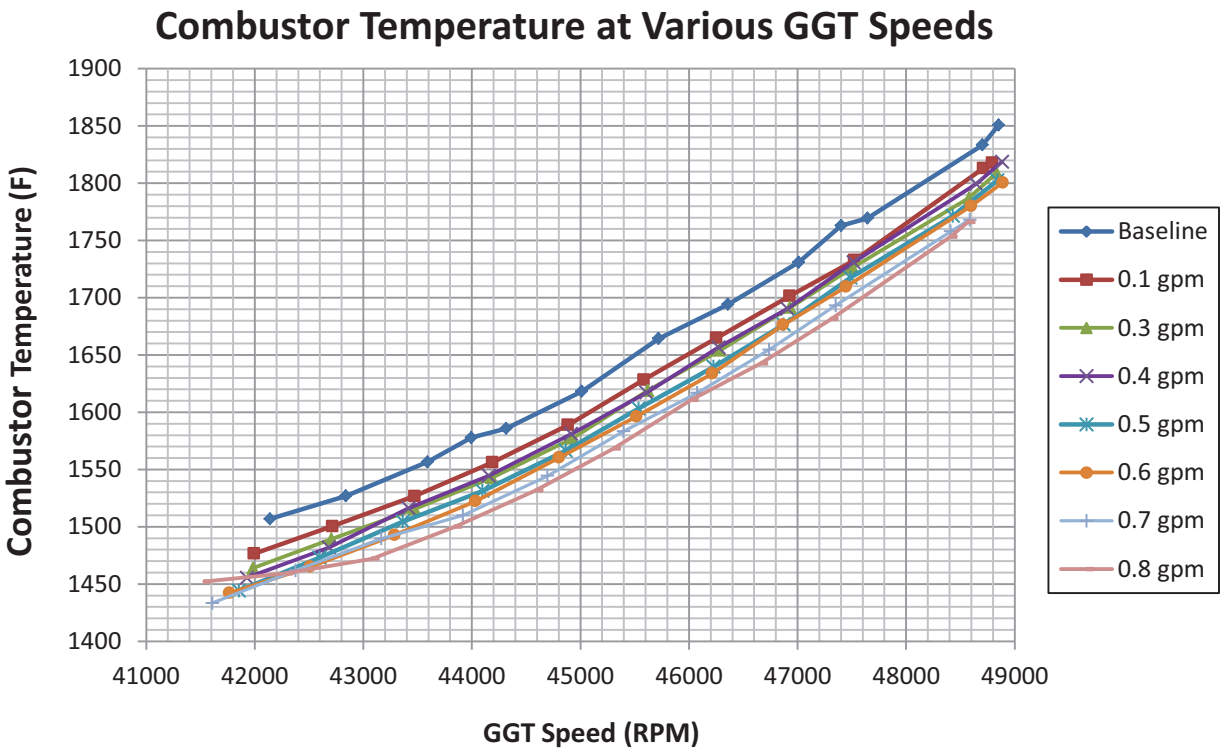

Figure 34: Combustor temperature with water spray at various GGT speeds

Spraying water into the compressor discharge caused approximately a 100ºF reduction in combustor temperature for the greatest water spray flow rate, 0.8 gpm. Increasing the water mass flow rate reduced the combustor temperature corresponding to a specific GGT speed.

Figure 34 also provides insight into how the engine controls fuel flow. For each water spray test, lower combustor temperatures corresponded to slower GGT speeds. Once water was injected, the combustor temperature decreased and caused the GGT speed to drop below the

speed it would have operated at under baseline conditions. This reduction in GGT speed for a fixed throttle setting decreased the compressor speed and consequently the compressor discharge pressure. Through pneumatic connections, the power turbine governor sensed the drop in compressor discharge pressure for the given throttle setting, so it scheduled more fuel to the gas generator turbine to maintain the dynamometer shaft speed at 6000 rpm. This increase in fuel is evident in the trends previously displayed in Figure 31. Once the additional fuel entered the combustor, the reaction proceeded until it reached a mixing temperature with the water that fell between the baseline combustor temperature and the temperature the combustor would have been if no extra fuel were added. Figure 35 indicates the combustor temperatures that resulted from various fuel flow rates and water spray flow rates. Data are shown starting at the fuel flow rate corresponding to the start of the water spray at 80% throttle.

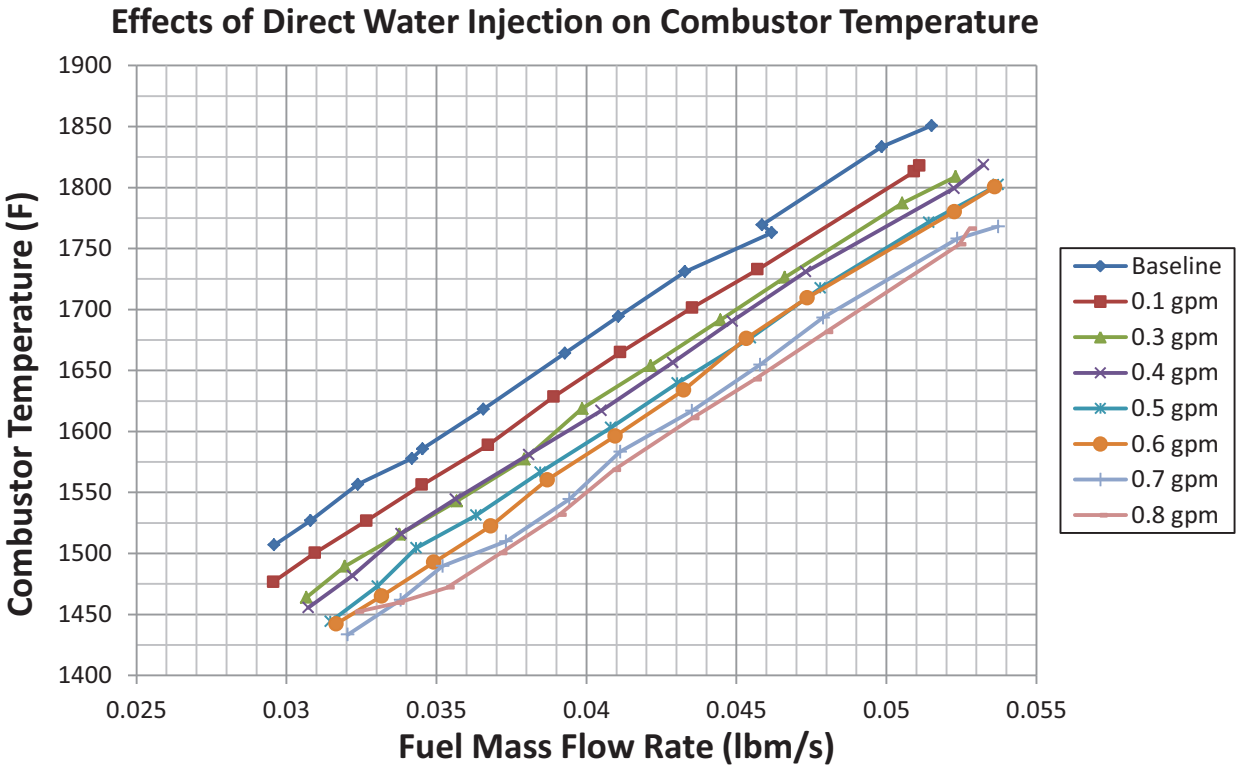

Figure 35: Combustor temperatures at various fuel mass flow rates (lbm/s)

At a given throttle setting, the decrease in GGT speed caused the power produced by the

power turbine to decrease since the water brake did not need to exert as much force to keep the dynamometer shaft, and by extension the power turbine shaft, at a constant speed. In order to compensate for the reduced GGT speed, the governor scheduled more fuel to the engine. Increasing the fuel mass flow rate allowed the power turbine to produce more power at the expense of increased fuel consumption. Hence, the amount of fuel needed to attain a specific power output increased. As shown in Figure 36, for a specific power output, the fuel mass flow rate needed increased as the water spray flow rate increased.

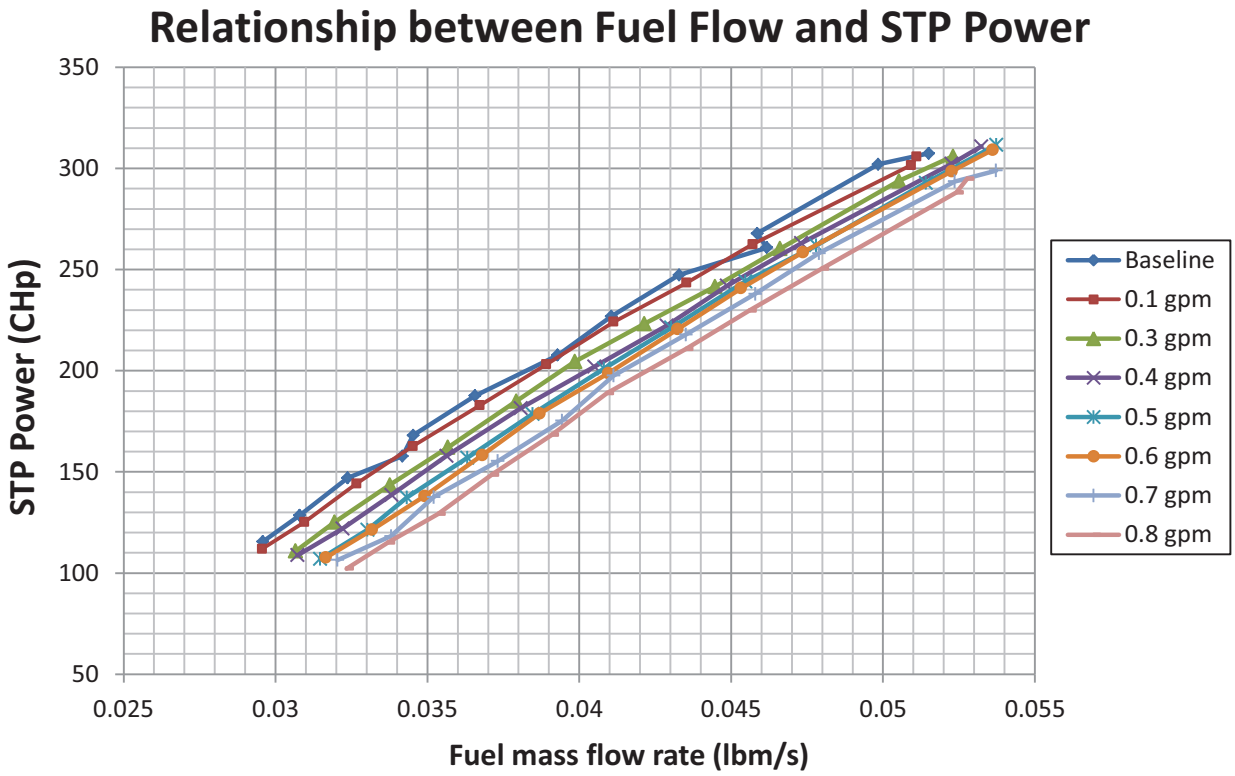

Figure 36: STP Power at various fuel flow rates and water flow rates

However, as previously shown in Figure 35, since the combustor temperature decreased for a specific fuel mass flow rate, the power output at a specific combustor temperature actually increased with increasing water spray. Although the power output decreased with water spray when compared with fuel mass flow rate, the combustor temperature decreased to a greater relative amount. **As a result, water injection at the compressor discharge allowed greater**

power output to be attained at lower combustor temperatures than the baseline conditions. The effect of post-compression water injection on the corrected power output at specific combustion temperatures is shown in Figure 37. Data are shown starting at the 80% throttle temperatures.

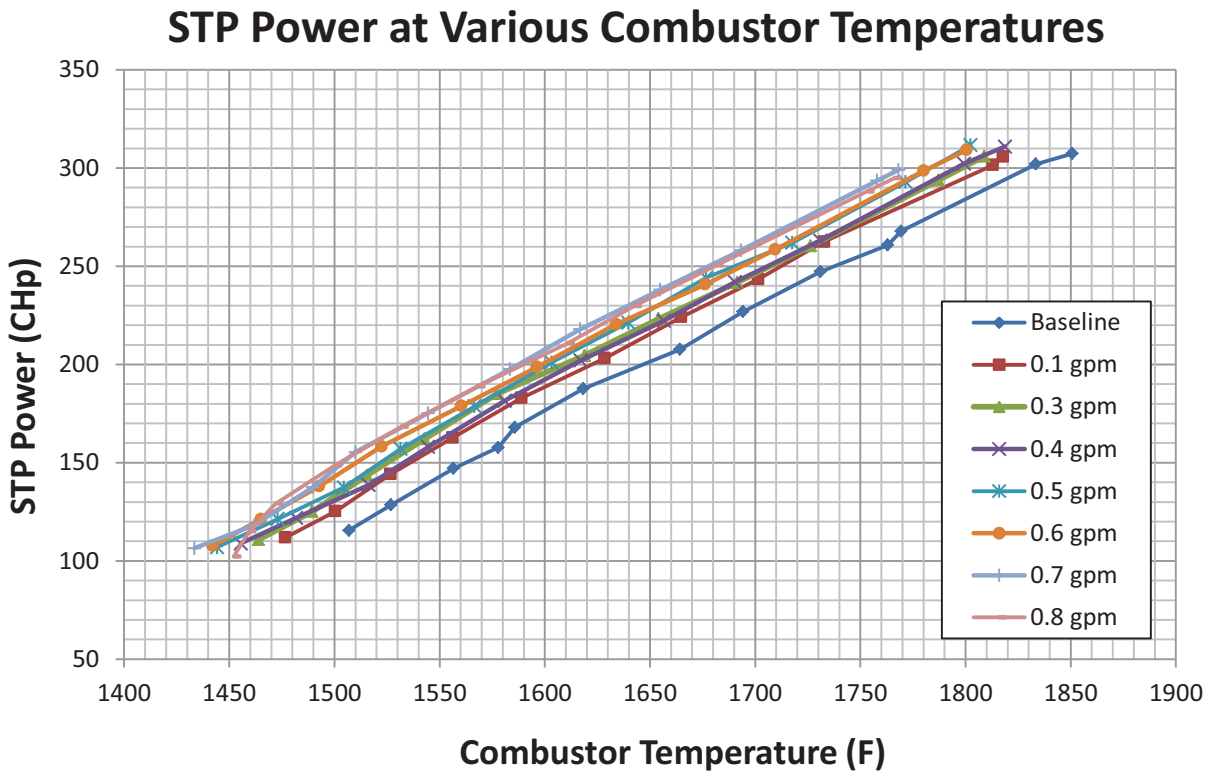

Figure 37: STP Power at specific combustion temperatures with water injection

As Figure 37 indicates, water injection at the compressor discharge yielded greater power output for a specific combustor temperature as the water spray volume increased. Operating at 1700°F, which corresponded to approximately 90% throttle, the turbine produced 270 Hp with 0.8 gpm spray compared to 230 Hp without the spray. The 40 Hp increase represented a 17% increase in power output at a specific combustor temperature from injecting water at the compressor discharge. Since turbine blade melting temperatures are limiting factors for engine design, being able to produce more power at lower operating temperatures can be very beneficial for engine operators. However, in order to fix the combustor temperature and achieve the observed power

increases, the engine would need a different fuel governing schedule than what it was originally designed with.

Examination of the power output in relation to the corrected air mass flow rate yielded less distinct results than those of the power output compared to the combustor temperature. Figure 38 shows the relationship between corrected power output and corrected air mass flow rates for the various water spray flow rates.

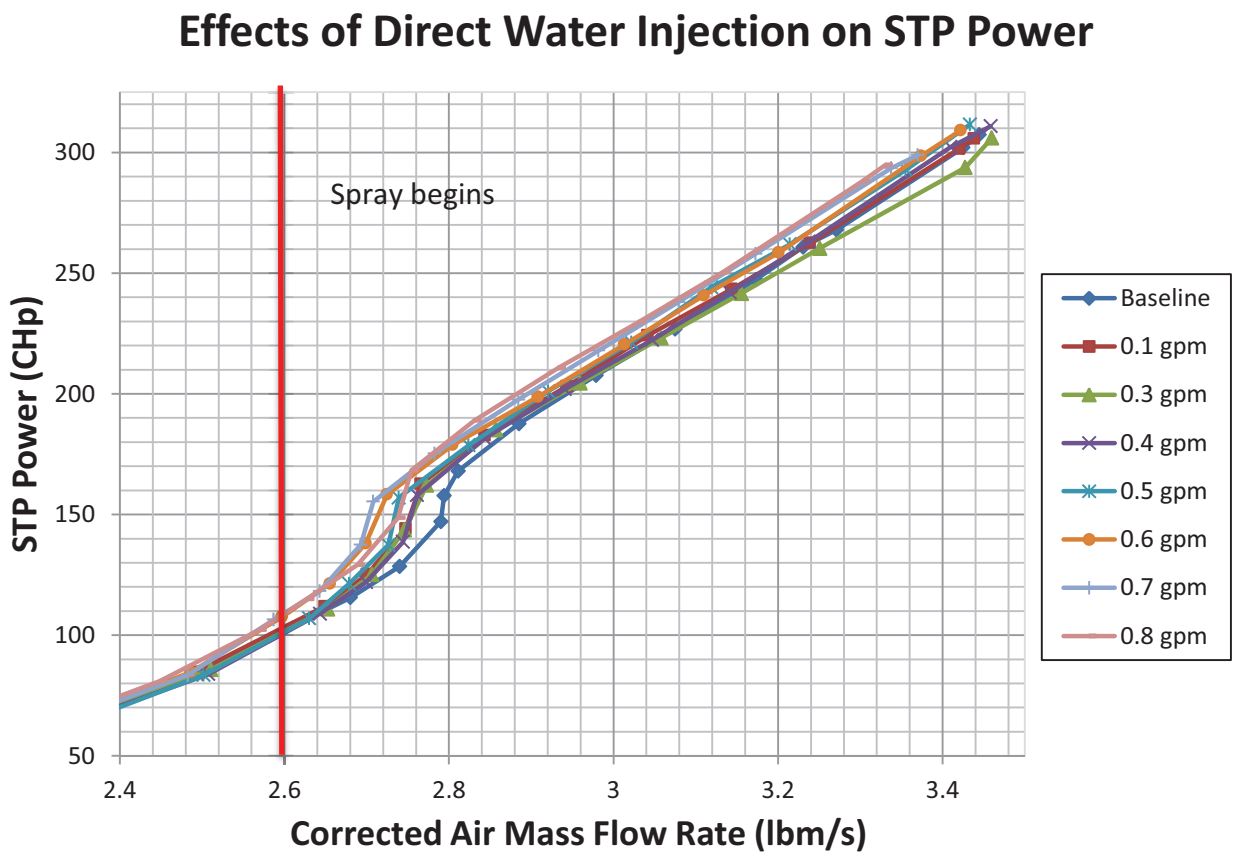

Figure 38: Corrected power output at various air mass flow rates

It appeared that water injection slightly increased power output at a specific air mass flow rate, but upon comparison with the plot of baseline runs versus the corrected air flow as shown in Figure 27, some of the observed increases in power output could be attributed to fluctuations in the atmospheric conditions on the days of the tests. As a result, although it appeared that post-

compression water injection may have increased power output at specified air mass flow rates, the data were not conclusive enough to ascertain the true magnitude of that increase.

However, given the large body of evidence indicating an increase in fuel flow rate as a result of water injection, it appeared that water injection at the compressor discharge increased power output at a specific combustor temperature at the expense of increased fuel consumption. Figure 39 displays the effect of water injection on brake specific fuel consumption, a measure of the fuel consumed in relation to the power generated. Data are displayed starting with the values corresponding to 80% throttle.

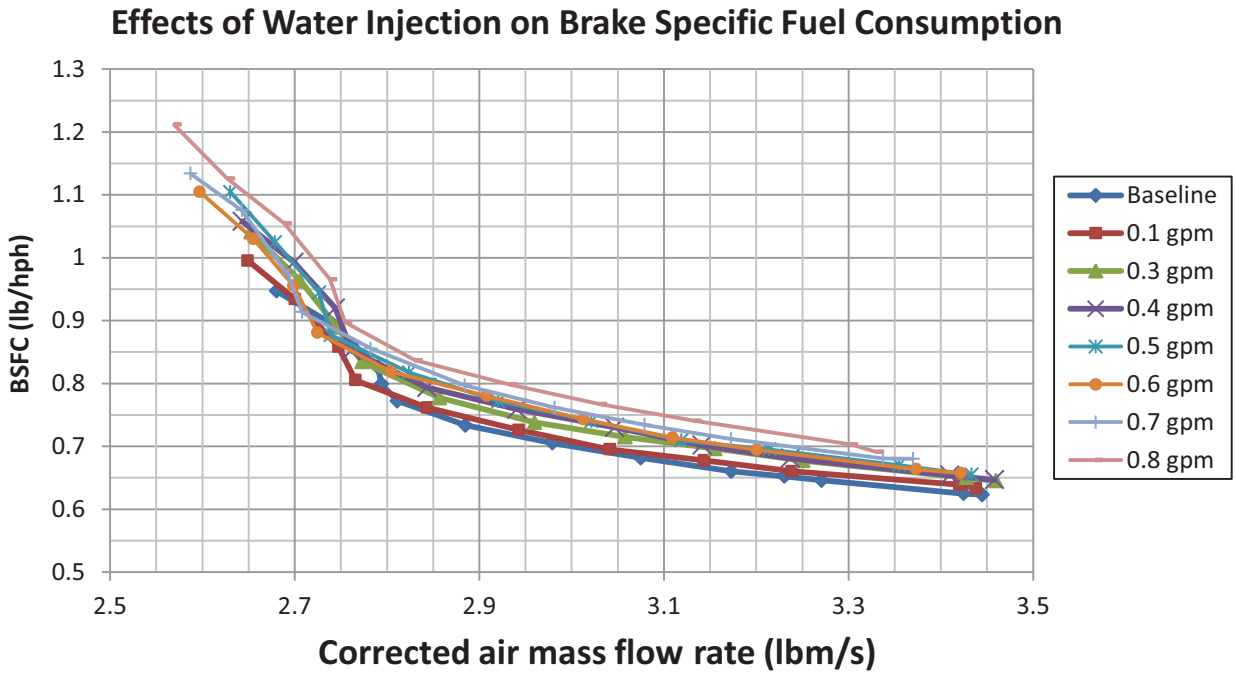

Figure 39: Effect of water injection on BSFC at various water flow rates

Although the increase was relatively small in magnitude, it indicated that the engine's fuel efficiency decreased as water was injected. Despite the penalties to fuel efficiency, water injection significantly reduced thermal NO_x emissions. Thermal NO_x emissions are dependent on the combustor temperature, so cooling the combustor by injecting water at the compressor discharge was very effective at reducing the amount of nitric oxides formed. Although water

injection reduced NO_x emissions, it also increased the concentration of unburned hydrocarbons (UHC) since the lower combustor temperature prevented all of the reactants from combusting. Figure 40 shows the decrease in thermal NO_x emissions for a specific air mass flow rate while Figure 41 shows the corresponding increase in concentration of unburned hydrocarbons at the same specific air mass flow rates. The data were shifted to account for differences in baseline NO_x and UHC concentration measured by the gas analyzer throughout the runs. As both figures demonstrate, increasing the water flow rate reduced the NO_x emissions from the baseline by over 50% at the highest water flow rate, but increased the concentrations of unburned hydrocarbons.

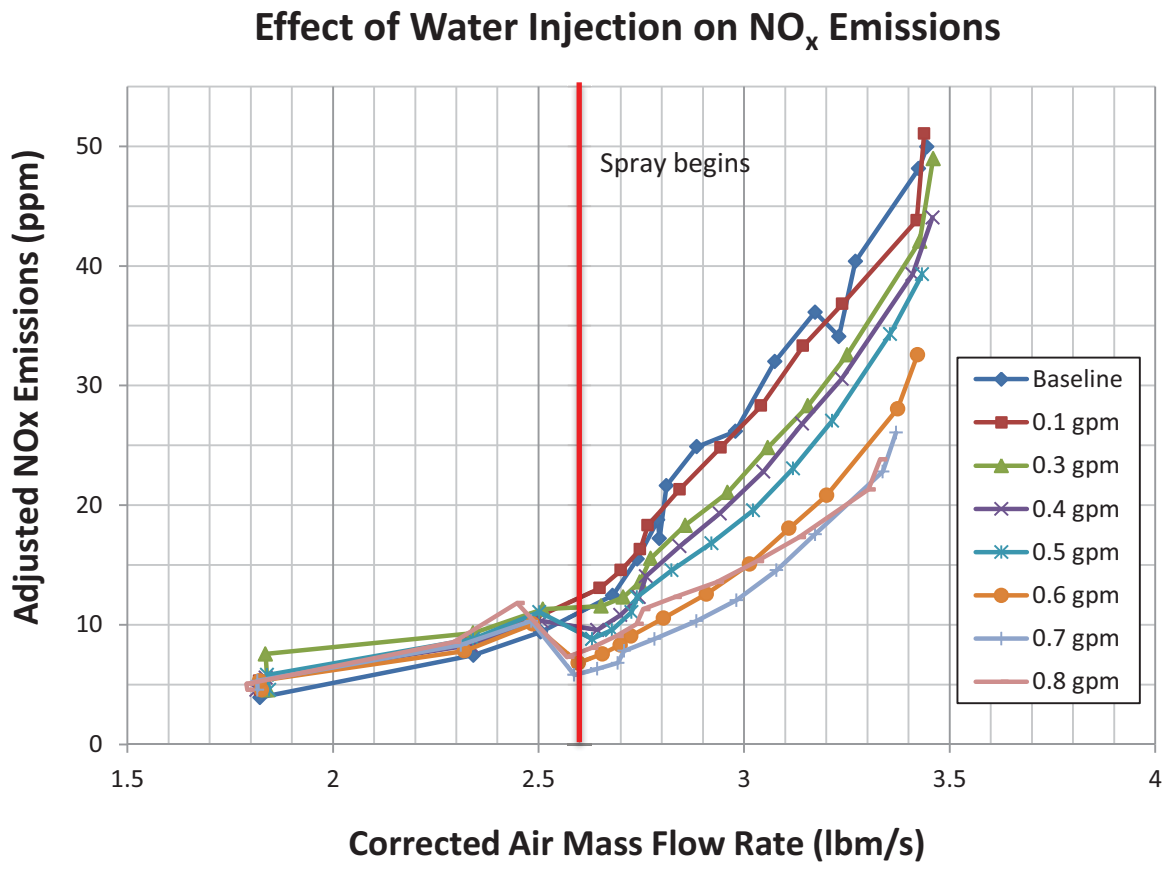

Figure 40: NO_x emissions with water injection

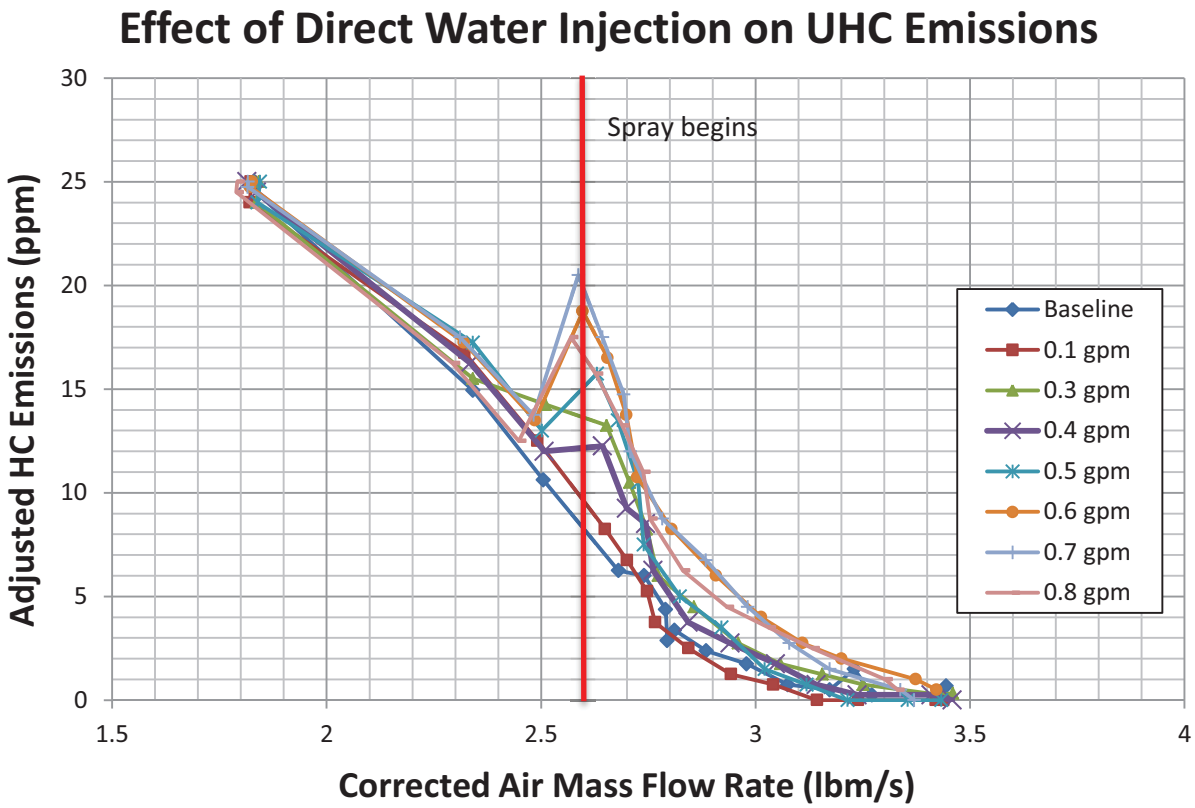

Figure 41: UHC emissions with water injection

6.2.2. Effects of Varying Water Temperature on Engine Performance and Emissions

As observed in the theoretical analysis, altering the water temperature was not expected to significantly change power output or other performance characteristics of the Rolls-Royce M250. This prediction was corroborated in the testing and the negligible effect of increasing water temperature on the turbine performance is shown in Figure 42.

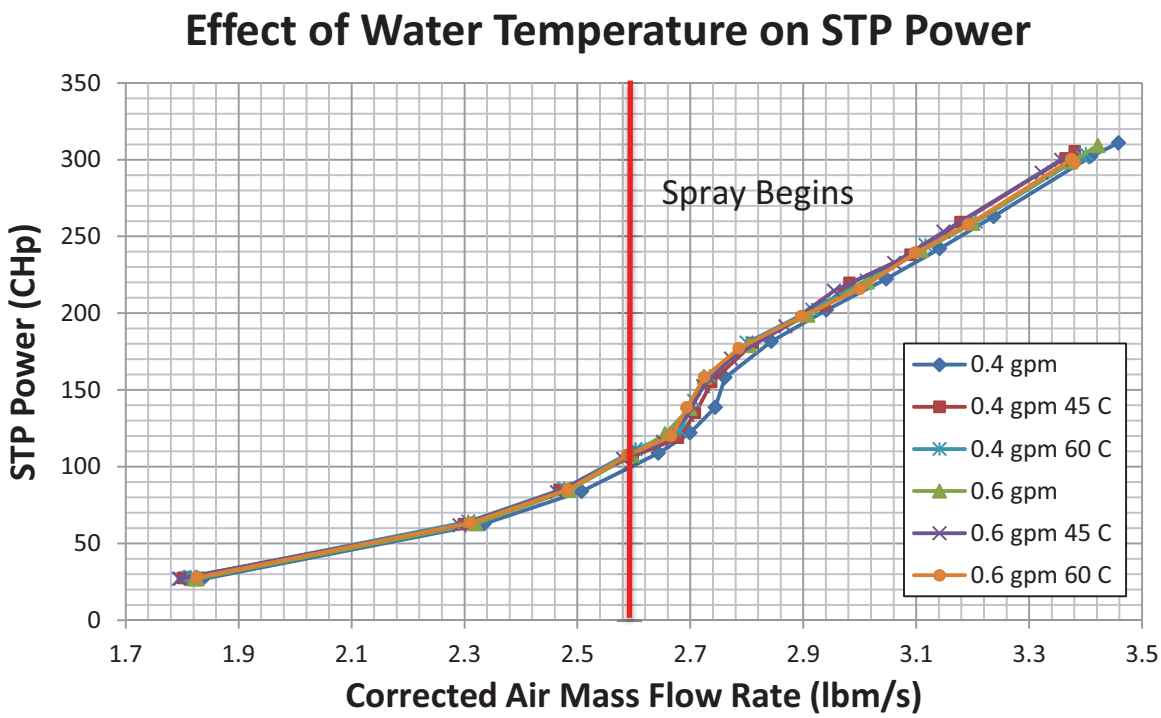

Figure 42: Effect of water temperature on power output

Water temperature tests were primarily conducted to determine if sensible heating would have any effect on the emissions results, which could not be accurately examined in the theoretical analysis. Figures 43 and 44 show that for the most part, changing water temperature did not have a significant impact on the NO_x and unburned hydrocarbon emissions. Although it appears that increasing the water temperature may have slightly reduced the NO_x emissions at each of the two flow rates tested, it is not conclusive how much of the observed NO_x effects could be attributed to uncertainty in the Five Gas Analyzer readings. Similarly, although increasing the water temperature seemed to have increased the concentrations of unburned hydrocarbons in some instances, the contribution of uncertainty to the observed levels made drawing conclusions regarding the effects of the water temperature difficult.

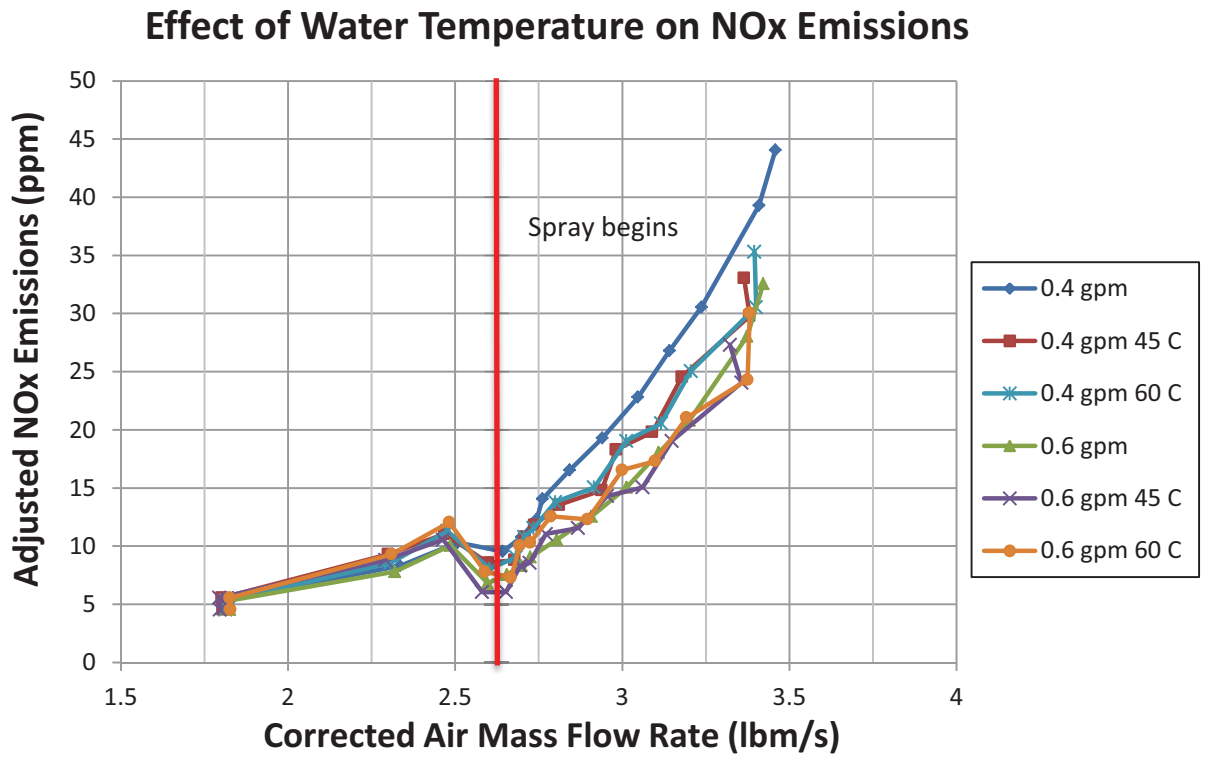

Figure 43: NO_x emissions with varying water temperature

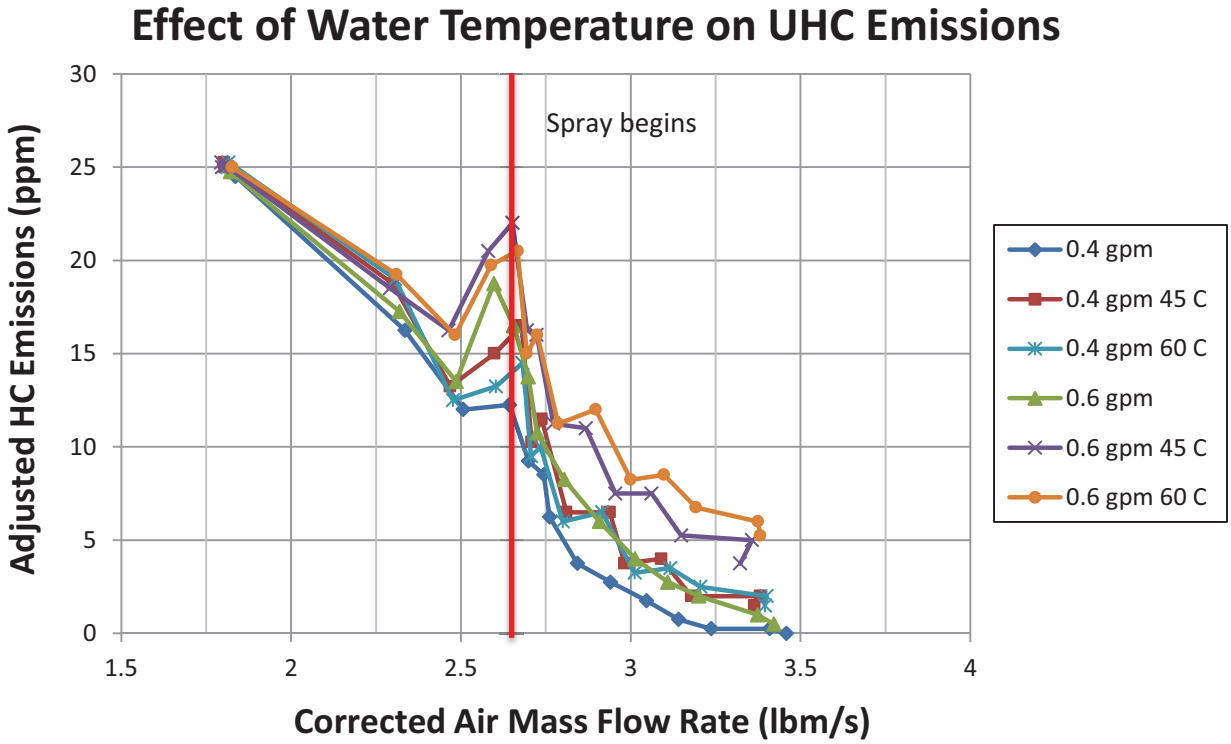

Figure 44: UHC emissions with varying water temperature

6.3. Comparison of Select Results with Inlet Fogging Data

Although the project originally intended to conduct tests on Gas Turbine #1 in the Rickover Gas Turbines Lab, the same gas turbine engine that Daniel Golden conducted compressor inlet fogging tests on in Trident Project #367, a servo motor control malfunction on Gas Turbine #1 prevented the tests from occurring. The project had to be conducted on Gas Turbine #2 instead, which produced less power than Gas Turbine #1 and generated a maximum pressure ratio of 6 compared to the pressure ratio of 7 of Gas Turbine #1. As a result, direct comparison of the results of post-compression water injection and compressor inlet fogging was not possible. However, select data from each of the projects was normalized based on the baseline operating conditions of each engine to give an indication of the effects of each water injection method on the particular engine that the tests were conducted on. Figure 45 shows the effect of post-compression water injection on the corrected power output compared to the baseline condition at various throttle settings.

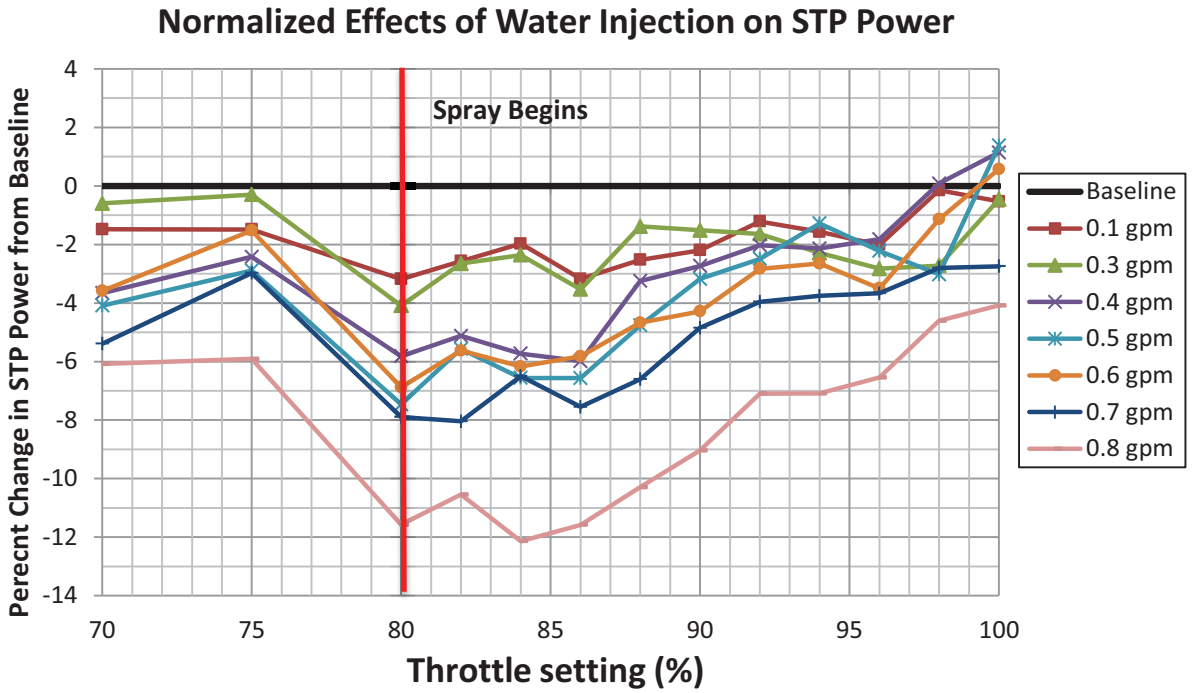

Figure 45: Normalized post-compression water injection power data

The normalized corrected power data for post-compression water injection shows that at a specific throttle setting, the water spray decreased the power output compared to the baseline by up to 12% at the most extreme point of the various flow rates. This decrease in power for a specific throttle setting was expected since the water cooled the combustor products, reducing the flame temperature of the product gases.

In the compressor inlet fogging experiments, the water reduced the amount of work that the compressor had to perform by increasing the density of the inlet air. Although inlet fogging decreased the combustor products temperature just as post-compression injection did, it also reduced the work that the GGT had to perform to operate the compressor, leaving more energy in the product gases to reach the power turbine. Due to the reduced compressor work, the power output from the compressor inlet fogging experiments largely demonstrated smaller reductions in power at each throttle setting compared to the normalized post-compression water injection results. The normalized power results of the inlet fogging experiments are shown in Figure 46.

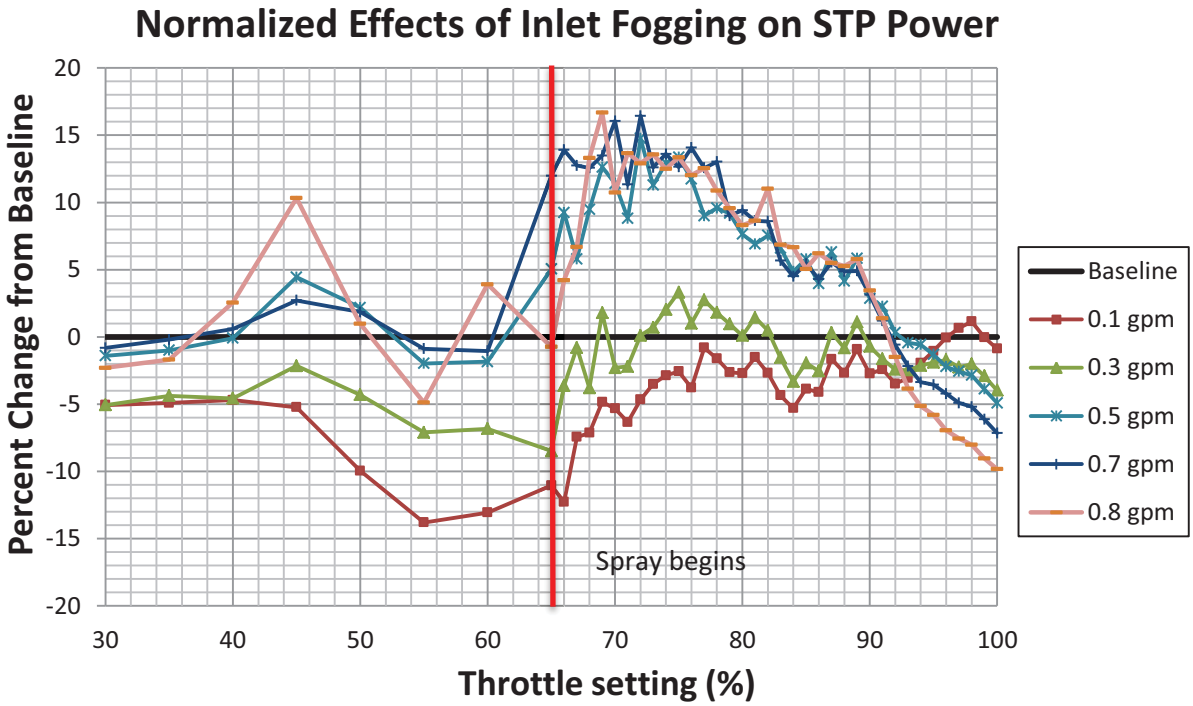

Figure 46: Normalized inlet fogging power results at various throttle levels

As Figure 46 shows, the higher water flow rates even appeared to yield relative increases in power at some throttle levels. However, these power increases may not be have been due to inlet fogging since the inlet fogging spray was activated at around 65% throttle, before the bleed air valve closed. As a result, data between 65% and 75% throttle for the inlet fogging experiments did not represent the full effects of the spray on engine performance. Some of the water spray that passed through the compressor was able to escape through the bleed air valve before ever reaching the combustion chamber. Additionally, from the maximum relative power output, most of the flow rates injected caused the power to decrease steadily as the throttle increased to 100%. At 100% throttle, the 0.8 gpm inlet fogging test actually exhibited twice as large of a relative decrease in power output as the 0.8 gpm post-compression water injection test.

With some exceptions, inlet fogging generally demonstrated greater improvements to engine performance compared to the baseline tests than post-compression water injection. The normalized results for brake specific fuel consumption supported this observation and are shown in Figures 47 and 48.

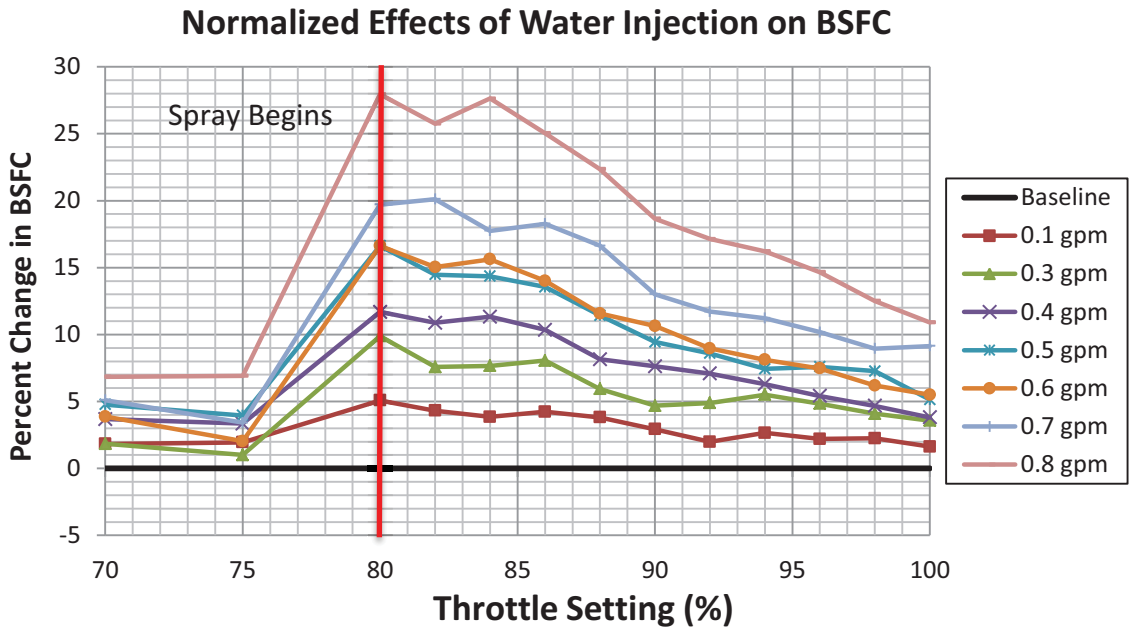

Figure 47: Normalized effects of water injection on BSFC

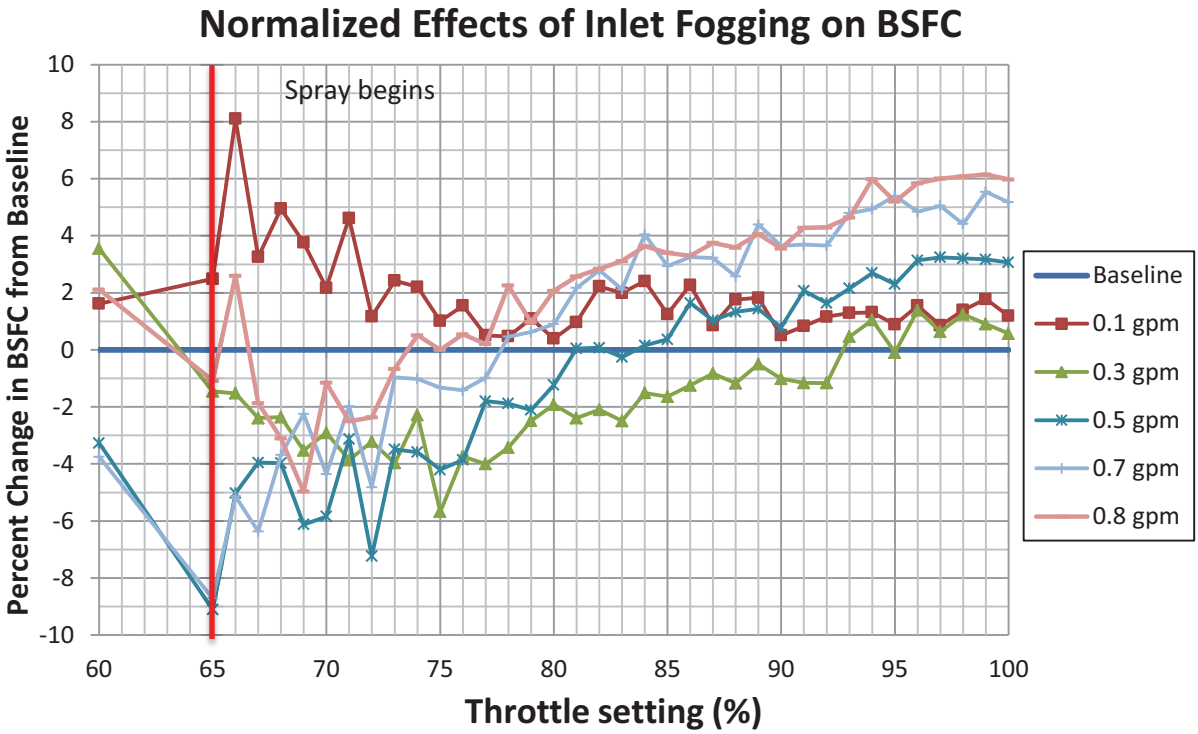

Figure 48: Normalized effects of inlet fogging on BSFC

As Figure 47 indicated, post-compression water injection caused the brake specific fuel consumption to increase for all flow rates. The 0.8 gpm test yielded an 11% increase in fuel consumption over the baseline tests for 100% throttle. This result indicated that post-compression water injection reduced fuel efficiency as the water flow rate increased. The inlet fogging results likewise showed increases in fuel consumption at the higher throttle settings, but the magnitudes of the increases were smaller than for post-compression injection. For the 0.8 gpm inlet fogging flow rate, the brake specific fuel consumption increased by 6% over the baseline at 100% throttle, compared to the 11% for post-compression injection.

Normalized results for the combustor temperature for each spray showed greater reductions as a result of inlet fogging compared to post-compression water injection. Figures 49 and 50 show the normalized combustor temperature results for post-compression water injection and inlet fogging, respectively.

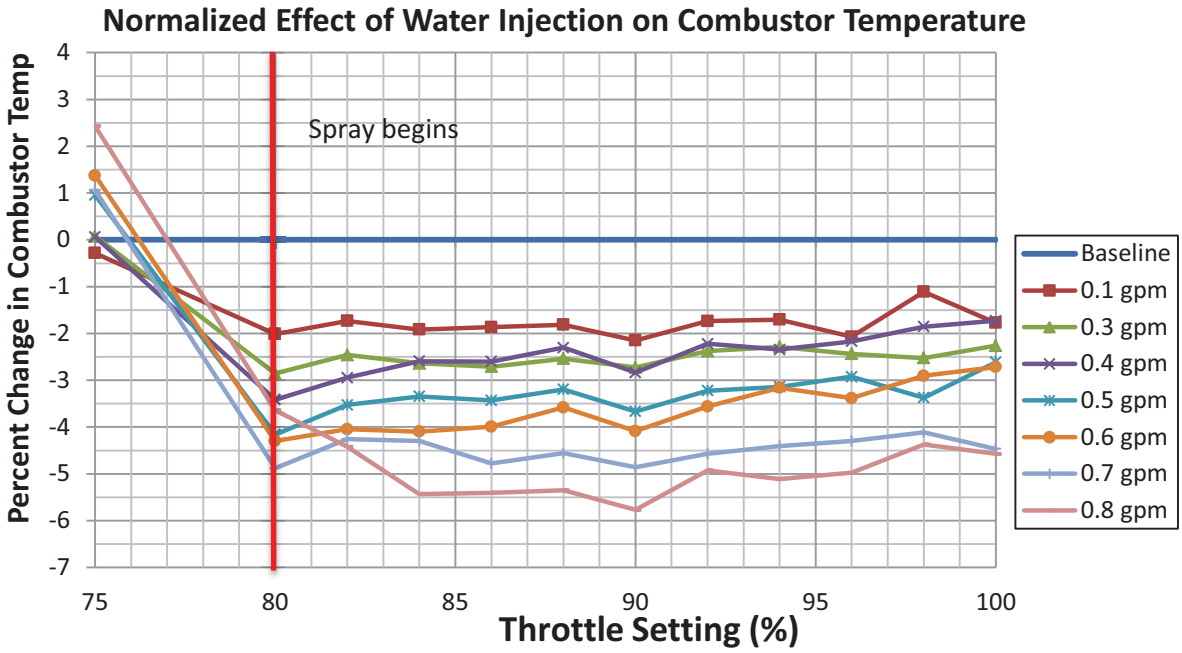

Figure 49: Normalized effect of water injection on combustor temperature

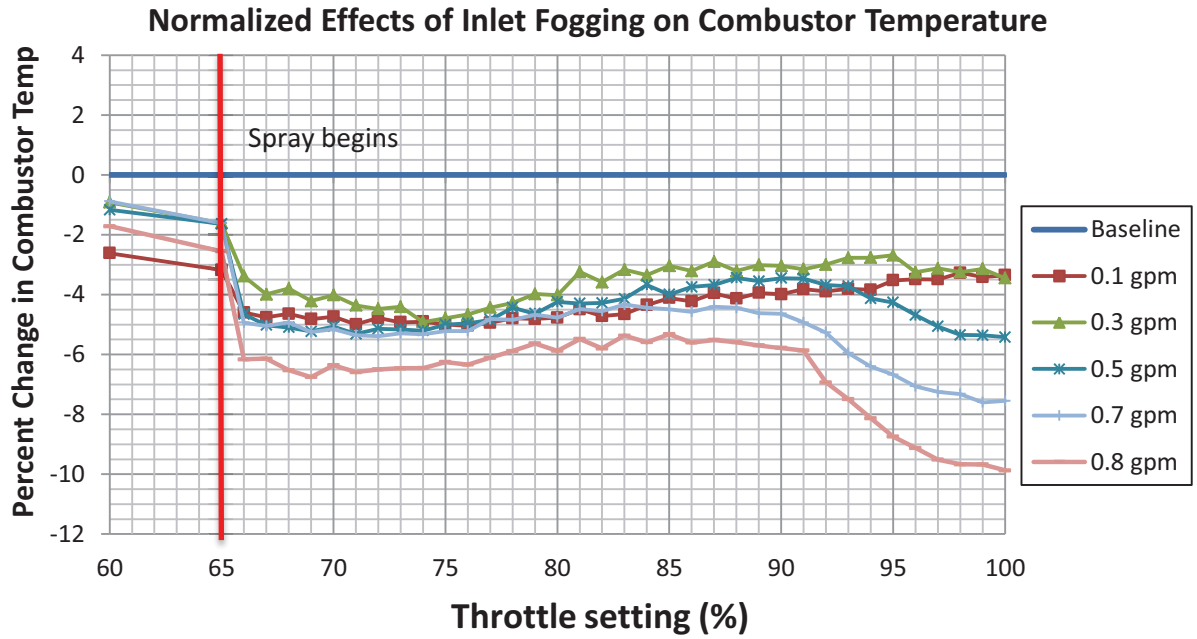

Figure 50: Normalized effect of inlet fogging on combustor temperature

The normalized results of water injection for combustor temperature showed a percent reduction from the baseline of 5.5% at the 100% throttle setting. This relative change is smaller in magnitude than that of inlet fogging, which produced a percent reduction of 10% at the 100%

throttle setting. Based on the normalized combustor temperature results, it appeared that inlet fogging was more effective at reducing the combustor temperature compared to the baseline conditions. For the three engine performance characteristics for which normalized comparisons were conducted, it appeared that inlet fogging generally yielded greater magnitudes of relative improvement than post-compression water injection. Although post-compression water injection demonstrated a smaller reduction in power output at 100% throttle, inlet fogging yielded a smaller increase in brake specific fuel consumption and a greater reduction in combustor temperature, which directly affected NO_x emissions. Overall, post-compression water injection yielded similar effects on engine performance compared to inlet fogging without exposing the compressor to liquid water.

7. CONCLUSIONS

Post-compression water injection produced significant effects on the performance, operating characteristics, and emissions of the Rolls-Royce M250. For a specific combustion temperature, injecting water at the compressor discharge increased the power output by around 20% from the baseline levels for the 0.8 gpm water spray test (3.2% of air flow by mass). All other water spray tests also increased the power output to a lesser degree. Furthermore, all of the water spray tests reduced the NO_x emissions, with the 0.8 gpm test yielding the greatest reduction at over 50%. These benefits came at the expense of reduced fuel efficiency, as demonstrated by an increase in brake specific fuel consumption for each of the water spray runs. Additionally, the reduced combustor temperatures caused by the water injection caused slightly elevated levels of unburned hydrocarbons due to incomplete combustion.

While simply spraying water into the turbine yielded appreciable results in terms of engine performance and emissions, altering the sensible water temperature did not seem to

produce much of an effect on either parameter. Based on the theoretical analysis, increasing the temperature should not have caused any significant changes to power output, and the data reinforced the predictions. Additionally, although changing water temperature exhibited potential effects on emissions, there was not enough conclusive evidence to distinguish the data trends from what might have been uncertainty in the measurements.

Comparison of the post-compression water injection data with compressor inlet fogging data was an initial goal of the project, but unforeseen complications with the original gas turbine engine that was to be studied caused the tests to be conducted on another gas turbine. The new gas turbine engine had different operating characteristics than the original, making comparison of results between the two difficult to interpret. However, normalization of the data to the baseline runs was conducted in order to attempt to identify any relationships between the two water injection methods. The normalized data indicated that post-compression water injection largely caused greater relative changes compared to the baseline condition than compressor inlet fogging. Most of these changes indicated that compressor inlet fogging may be a more preferable method of water injection based on the performance results.

However, post-compression injection yielded comparable results throughout the range of throttle settings during which the spray was activated without having to inject water into the compressor. Unlike compressor inlet fogging, which risks reducing compressor component life by exposing the compressor blades to liquid water droplets, post-compression water injection ensures that the water is fully vaporized by the time it reaches its first turbine blades at the gas generator turbine. As such, post-compression water injection may be a more prudent alternative to compressor inlet fogging for low pressure-ratio gas turbine applications if the risk of reduced engine life is a concern.

Although water injection at the compressor discharge demonstrated the potential for increased power output at specific combustor temperatures and air flow rates, practical application of post-compression water injection in systems that utilize small gas turbines like the Rolls-Royce M250 may be difficult. If water is not readily available at the gas turbine installation, water tanks would need to be used that could pose problems to system weight and effectiveness. For optimal engine life, the water should also be purified to prevent contaminants in the spray from damaging the engine components. Depending on how easily a water injection system could be incorporated into an existing gas turbine engine and whether there is a need for either reduced emissions or increased power output, post-compression water injection may not be a viable option for many small gas turbines.

For the future, additional studies are recommended to investigate the effects of steam augmentation on low-pressure ratio gas turbines such as the Rolls-Royce M250. Although steam requires much more energy than heated water to produce, it yields similar effects to power and emissions as simple water injection while increasing system efficiency. With the Navy's increased focus on shipboard waste heat recovery systems, steam augmentation could be implemented on ships using a waste heat recuperator to superheat the injected water [15]. Much of the energy released by the fuel in a gas turbine engine is lost as heat rejected to the environment. If even half of that energy could be reclaimed, substantial energy savings would result. Using steam injection in gas turbines in conjunction with a recuperation system would allow ships to provide increases in electrical power generation or propulsion with no additional heating cost. Steam injection would also reduce the level of NO_x emissions, helping the Navy make progress towards its environmental stewardship initiatives [16]. Understanding the effects of both compressor inlet fogging and post-compression water injection on gas turbines provides

a better understanding of the effects of any water-injected system, including steam, on engine operations. Insight gained from water injection research allows more detailed research into the incorporation of more advanced steam-injected gas turbine systems for military and civilian applications.

References

[1] Langston, Lee S., and George Opdyke, Jr. "Introduction to Gas Turbines for Non-Engineers." Global Gas Turbine News 37.2 (1997): n. pag. ASME. American Society of Military Engineers. Web. 26 Dec. 2013.

[2] United States. Navy. Naval Energy Office. *Naval Energy: A Strategic Approach*. Office of the Secretary of the Navy: Washington, D.C., October 2009. Print.

[2] Meacock, A. J., and A. J. White. "The Effect of Water Injection on Multispool Gas Turbine Behavior." *Journal of Engineering for Gas Turbines and Power* 128.1 (2004): n. pag. *ASME Digital Collection*. Web. 20 Mar. 2014.

[4] Hasselbacher, Hermann. "Performance of Water/steam Injected Gas Turbine Power Plants Consisting of Standard Gas Turbines and Turbo Expanders." *International Journal of Energy Technology and Policy* 3.1-2 (2005): 12-23. Web. 21 Mar. 2014. http://www.environmental-expert.com/Files%5C6471%5Carticles%5C6373%5Cf319685411122710.pdf.

[5] Daggett, David L., Silvio Ortanderl, David Eames, Jeffrey J. Berton, and Christopher A. Snyder. *Revisiting Water Injection for Commercial Aircraft*. Tech. no. 2004-01-3108. Reno: SAE International, 2004. Print.

[6] Chaker, Mustapha, Cyrus B. Meher-Homji, and Thomas Mee, III. "Inlet Fogging of Gas Turbine Engines-Part I: Fog Droplet Thermodynamics, Heat Transfer, and Practical Considerations." *Journal of Engineering for Gas Turbines and Power* 126.July (2004): 545-47. Print.

[7] Mohan, S. Paul, Robert D. Underwood, and David A. Little. "Design, Installation, and Test of a Steam Injection System on an Early Frame 3 Gas Turbine in a Combined Cycle Pipeline Compressor Station." *Proceedings of the Twenty-First Turbomachinery Symposium*. Twenty-First Turbomachinery Symposium. 137-50. *Proceedings of the Twenty-First Turbomachinery Symposium*. Web. 30 Jan. 2014.

[8] Samaras, Christos. "Emissions Reduction In Conventional Gas Turbine Combustors." *My Engineering World*. N.p., 5 Dec. 2012. Web. 23 Mar. 2014. <http://www.myengineeringworld.net/2012/12/emissions-reduction-in-conventional-gas.html>.

[9] Brun, Klaus and Rainer Kurtz. “Gas Turbine Life Limiting Effects of Inlet and Interstage Water injection.”

[10] Daggett, David L., Silvio Ortanderl, David Eames, Jeffrey J. Berton, and Christopher A. Snyder. *Revisiting Water Injection for Commercial Aircraft*. Tech. no. 2004-01-3108. Reno: SAE International, 2004. Print.

[11] Urbach, Herman B., Donald T. Knauss, Balfour L. Wallace, John Emory, John Frese, and Joseph W. Bishop. Water Injection into Navy Gas-Turbine Combustors to Reduce NOx Emissions. Tech. no. 074-0188. Washington, D.C.: Office of Management and Budget, n.d.

Print.

[12] Brooks, Frank J. *GE Gas Turbine Performance Characteristics*. Publication no. GER-3567H. N.p.: n.p., n.d. GE Power Systems. Web. 04 Feb. 2014.

[13] Golden, Daniel L. *An Experimental Study of Water Injection into a Rolls-Royce Model 250- C20B Turboshaft Gas Turbine*. Rep. no. 367. Annapolis, MD: US Naval Academy, 2008. Print.

[14] Chaker, Mustapha, Cyrus B. Meher-Homji, and Thomas Mee, III. "Inlet Fogging of Gas Turbine Engines-Part I: Fog Droplet Thermodynamics, Heat Transfer, and Practical Considerations." *Journal of Engineering for Gas Turbines and Power* 126.July (2004): 547-49. Print.

[15] Putnam, Dean. *Gas Turbine Engine Exhaust Waste Heat Recovery Shipboard Module Development*. NAVSEA, n.d. Web. 23 Mar. 2014. <http://www.navysbir.com/n10_3/N103-229.htm>.

[16] Amy, John V., Jr. *The Department of the Navy's Research Development and Acquisition Community Efforts to Achieve the Navy's Energy Goals*. N.p.: Office of the Secretary of the Navy, Mar. 2011. PDF.

Appendix A: Theoretical Water Injection Model

```
"Water injection calculations"
"Brian He"
"2014-2015"

"Assumed no pressure losses after water injection. Modeled air as a dry ideal gas. Used variable specific heats. Obtained raw data values from previous gas turbines lab. Assumed water and air are at same pressure and temperature."
"Throttle = 100%"

"Constants"
eta_pt = 0.904082                                   {from gas turbines data}
k = 1.40
Tw_0 = 60 [F]
Pw_0 = 1*convert(atm,psia)
rho_w = Density(water,T=Tw_0,P=Pw_0)

"Variables"
{m_dot_air  = 1  [lbm/s]}
{Tw=100 [C]}
m_dot_w = 0.1*convert(gpm,m^3/s)*rho_w               "Units: lbm/s"

"1: Compressor Inlet"
Pa_1 = 14.75 [psia]                                 "Assumed constant"
Ta_1 = 65 [F]                                       "Assumed constant"
ha_1 = enthalpy(Air,T=Ta_1)
sa_1 = entropy(Air,T=Ta_1,P=Pa_1)

"2: Compressor Discharge: Air side pre-mixing"
{P2base = 1}                                        "Obtained from baseline gas turbine data"
Pa_2 = P2base + Pa_1                                "Changes depending on throttle setting"
rp = Pa_2/Pa_1

eta_comp = 0.828                                    "Assumed constant compressor efficiency between throttle settings 80-100% for purpose of calculations"
has_2 = enthalpy(air,P=Pa_2,s=sa_1)
eta_comp = (has_2 - ha_1)/(ha_2 - ha_1)             "Used compressor efficiency to calculate Ta[2], air temperature after compressor"
Ta_2 = temperature(air,h=ha_2)

W_dot_comp = m_dot_air*(ha_2 - ha_1)                "Theoretical compressor work using compressor efficiency = 82.8%"

"2: Compressor Discharge: Water side pre-mixing"
m_dot_mix = m_dot_air + m_dot_w
Pw_2 = 250 [psia]
hw_2 = enthalpy(water,T=Tw_0,P=Pw_2)

"2-3: Air and water mole fractions"
n_air=m_dot_air/29.9                                "mole number, MW = 29.9"
n_w=m_dot_w/18                                      "mole number, MW = 18"
n_tot = n_air + n_w
y_air = n_air/n_tot                                 "air mole fraction"
y_w = n_w/n_tot                                     "water mole fraction"
```

```
"2-3: Mixing Process Case 1 - Assume Pa[3] is constant"
Pmix_3 = Pa_3 + Pw_3
Pa_3 = Pa_2
Pw_3 = Pmix_3*y_w                                    "Solves for total pressure, Pmix and
subsequently water partial pressure, Pw"

{"2-3: Mixing Process Case 2 - Assume Pmix[2] is constant"
Pmix_3=100 [psia]
Pa_3=y_air*Pmix_2
Pw_3=Pmix_3*y_w}

"3: Compressor Discharge"
m_dot_air*ha_2 + m_dot_w*hw_2 = m_dot_air*ha_3 + m_dot_w*hw_3 "Energy balance assuming
adiabatic mixing"
ha_3 = enthalpy(air, T=Tmix_3)                       "Solves for Tmix"
hw_3 = enthalpy(water, T=Tmix_3, P=Pw_3)

hmix_2 = (m_dot_air*ha_2+m_dot_w*hw_2)/m_dot_mix   "Enthalpy of combined air-water entities
immediately before mixing"
hmix_3 = (m_dot_air*ha_3+m_dot_w*hw_3)/m_dot_mix   "Enthalpy of air-water mixture"
sa_2=entropy(air, T=Ta_2,P=Pa_2)
sa_3=entropy(air,T=Tmix_3, P=Pa_3)
sw_2=entropy(water, T=Tw_2, P=Pw_2)
sw_3=entropy(water,T=Tmix_3, P=Pw_3)
s_prod=m_dot_air*(sa_3-sa_2)+m_dot_w*(sw_3-sw_2)   "Checks 2nd Law"

"4: Combustor Exit"

"Solve for adiabatic flame temperature separate from water injection"

"Balanced stoichiometric reaction:"
{C12H26 + 18.5(O2 + 3.76N2) --> 12CO2 + 13H2O + 69.56N2}

"Complete combustion with varying air-fuel ratios; non-stoichiometric:"
{wC12H26 + x(O2+3.76N2) --> yCO2 + zH2O + qO2 + rN2}
"AF_hat = 1"
w=1
12*w=y
26*w=2*z
2*x=2*y+z+2*q
2*3.76*x=2*r
x = AF_hat/4.76

"Assumed constant air-fuel ratios: 30,50,70,75,80,82,84,86,88,90,92,94,96,98,100%
106.4417857
106.0547619
99.315
94.754
89.276
86.85
83.82833333
80.88714286
79.09333333
76.57833333
74.238
```

```
72.61833333
70.99833333
69.225
69.06333333
66.3525
65.56222222"

"Compute the adiabatic flame temperature without water for each case. Fuel enters at 77 F and air mixture enters at Tmix_3"
"H_products = H_reactants for adiabatic"

"Reactants"
hf = -151538 [Btu/lbmol]
h_O2r = enthalpy(O2,T=Tmix_3)
h_N2r = enthalpy(N2,T=Tmix_3)

"Products"
h_CO2p = enthalpy(CO2, T=Ta_f)
h_H2Op = enthalpy(H2O, T=Ta_f)
h_O2p = enthalpy(O2, T=Ta_f)
h_N2p = enthalpy(N2, T=Ta_f)

hf + x*h_O2r + x*3.76*h_N2r = y*h_CO2p + z*h_H2Op + q*h_O2p + r*h_N2p

Cp_gas = 0.24                                   "Btu/(lbm-F), obtained from generic combustion product gases"
Cp_w = Cp(Water,T=Tmix_3,P=Pw_3)
m_dot_air*Cp_gas*Ta_f + m_dot_w*Cp_w = m_dot_air*Cp_gas*Tmix_4 + m_dot_w*Cp_w*Tmix_4
"Energy balance, finds Tmix_4"}

T_mix[4] = 2221 [R]
Pa_4 = Pa_3
Pmix_4 = Pa_4 + Pw_4
Pw_4 = y_w*Pmix_4
ha_4 = enthalpy(air,T=Tmix_4)
hw_4 = enthalpy(water,T=Tmix_4, P=Pw_4)
hmix_4 = (m_dot_air*ha_4 + m_dot_w*hw_4)/m_dot_mix

"5: GGT exit"
rp_ggt = 3.02                                   "Used average pressure ratio across ggt from baseline data"
Pa_5 = Pa_4/rp_ggt
Pmix_5 = Pa_5 + Pw_5
Pw_5 = y_w*Pmix_5                               "Need to recalculate water pressures"

W_dot_comp = m_dot_air*(ha_4 - ha_5) + m_dot_w*(hw_4 - hw_5)
ha_5 = enthalpy(air,T=Tmix_5)
hw_5 = enthalpy(water,T=Tmix_5, P=Pw_5)         "Solves for Tmix_5 first, then ha_5 and hw_5"
hmix_5 = (m_dot_air*ha_5 + m_dot_w*hw_5)/m_dot_mix
W_dot_ggt = m_dot_mix*(hmix_4 - hmix_5)         {currently calculated using known temperatures}

sa_5 = entropy(air, T=Tmix_5, P=Pa_5)
sw_5 = entropy(water, T=Tmix_5, P=Pw_5)
smix_5 = (m_dot_air*sa_5 + m_dot_w*sw_5)/m_dot_mix

"6: PT exit"
```

```
Pa_6 = 14.03 [psia]                                    "Assumed to be slightly less than atmospheric
due to vacuum effect of fan"
Pmix_6 = Pa_6 + Pw_6
Pw_6 = y_w*Pmix_6

smixs_6 = smix_5
smixs_6 = (m_dot_air*sas_6 + m_dot_w*sws_6)/m_dot_mix  {finds isentropic condition}
sas_6 = entropy(air,P=Pa_6,T=Tmixs_6)                  {splits isentropic mixture into components}
sws_6 = entropy(water,P=Pw_6, T=Tmixs_6)

has_6 = enthalpy(air,P=Pa_6,s=sas_6)
hws_6 = enthalpy(water,P=Pw_6,s=sws_6)
hmixs_6 = (m_dot_air*has_6 + m_dot_w*hws_6)/m_dot_mix

eta_pt = (hmix_5 - hmix_6)/(hmix_5 - hmixs_6)          {uses turbine efficiency to calculate actual
enthalpy}
hmix_6 = (m_dot_air*ha_6 + m_dot_w*hw_6)/m_dot_mix
ha_6 = enthalpy(air, T=Tmix_6)
hw_6 = enthalpy(water, P=Pw_6, T=Tmix_6)

"Heat rate and Power"
Q_in = hmix_4 - hmix_3                                 {heat rate during combustion}
Q_dot_in = m_dot_mix*Q_in

W_pt = hmix_5 - hmix_6                                 {work from power turbine}
W_dot_pt = m_dot_mix*W_pt

W_dot_net = W_dot_pt + W_dot_ggt - W_dot_comp

"Water heating energy"
T_supply = ConvertTEMP(C,R,10)
P_tank = 33.5 [psia]
h_supply = enthalpy(water,T=T_supply,P=P_tank)
Q_dot_w = m_dot_w*(hw[2]-h_supply) {this quantity assumed to be provided by a heat exchanger in a
theoretical cycle in order to neglect heating}

"Thermal Efficiency"
eta_th = W_dot_net/Q_dot_in

"Indicated Horsepower (IHP)"
IHP = W_dot_net*3600*convert(Btu/hr,hp)

"Brake horsepower (BHP)"
eta_mech = 0.88 {Obtained from previous gas turbines data}
BHP = IHP*eta_mech

"Brake Specific Fuel Consumption"
{m_dot_fuel = 203.5 [lb/h]} {At 100% throttle}
BSFC = m_dot_fuel/BHP

"Baseline Statistics"
W_net_base = 84.8 [Btu/lbm] {obtained from gas turbines data at 100% throttle}
W_dot_net_base = m_dot_air*W_net_base
W_dot_net_increase = (W_dot_net-W_dot_net_base)/W_dot_net_base * 100 "Appendix A"

"Water injection calculations"
```

```
"Brian He"
"2014-2015"

"Assumed no pressure losses after water injection. Modeled air as a dry ideal gas. Used variable specific heats. Obtained raw data values from previous gas turbines lab. Assumed water and air are at same pressure and temperature."
"Throttle = 100%"

"Constants"
eta_pt = 0.904082                                   {from gas turbines data}
k = 1.40
Tw_0 = 60 [F]
Pw_0 = 1*convert(atm,psia)
rho_w = Density(water,T=Tw_0,P=Pw_0)

"Variables"
{m_dot_air  = 1  [lbm/s]}
{Tw=100 [C]}
m_dot_w = 0.1*convert(gpm,m^3/s)*rho_w               "Units: lbm/s"

"1: Compressor Inlet"
Pa_1 = 14.75 [psia]                                 "Assumed constant"
Ta_1 = 65 [F]                                       "Assumed constant"
ha_1 = enthalpy(Air,T=Ta_1)
sa_1 = entropy(Air,T=Ta_1,P=Pa_1)

"2: Compressor Discharge: Air side pre-mixing"
{P2base = 1}                                        "Obtained from baseline gas turbine data"
Pa_2 = P2base + Pa_1                                "Changes depending on throttle setting"
rp = Pa_2/Pa_1

eta_comp = 0.828                                    "Assumed constant compressor efficiency between throttle settings 80-100% for purpose of calculations"
has_2 = enthalpy(air,P=Pa_2,s=sa_1)
eta_comp = (has_2 - ha_1)/(ha_2 - ha_1)             "Used compressor efficiency to calculate Ta[2], air temperature after compressor"
Ta_2 = temperature(air,h=ha_2)

W_dot_comp = m_dot_air*(ha_2 - ha_1)                "Theoretical compressor work using compressor efficiency = 82.8%"

"2: Compressor Discharge: Water side pre-mixing"
m_dot_mix = m_dot_air + m_dot_w
Pw_2 = 250 [psia]
hw_2 = enthalpy(water,T=Tw_0,P=Pw_2)

"2-3: Air and water mole fractions"
n_air=m_dot_air/29.9                                "mole number, MW = 29.9"
n_w=m_dot_w/18                                      "mole number, MW = 18"
n_tot = n_air + n_w
y_air = n_air/n_tot                                 "air mole fraction"
y_w = n_w/n_tot                                     "water mole fraction"

"2-3: Mixing Process Case 1 - Assume Pa[3] is constant"
Pmix_3 = Pa_3 + Pw_3
Pa_3 = Pa_2
```

```
Pw_3 = Pmix_3*y_w                                    "Solves for total pressure, Pmix and subsequently water partial pressure, Pw"

{"2-3: Mixing Process Case 2 - Assume Pmix[2] is constant"
Pmix_3=100 [psia]
Pa_3=y_air*Pmix_2
Pw_3=Pmix_3*y_w}

"3: Compressor Discharge"
m_dot_air*ha_2 + m_dot_w*hw_2 = m_dot_air*ha_3 + m_dot_w*hw_3 "Energy balance assuming adiabatic mixing"
ha_3 = enthalpy(air, T=Tmix_3)                       "Solves for Tmix"
hw_3 = enthalpy(water, T=Tmix_3, P=Pw_3)

hmix_2 = (m_dot_air*ha_2+m_dot_w*hw_2)/m_dot_mix   "Enthalpy of combined air-water entities immediately before mixing"
hmix_3 = (m_dot_air*ha_3+m_dot_w*hw_3)/m_dot_mix   "Enthalpy of air-water mixture"
sa_2=entropy(air, T=Ta_2,P=Pa_2)
sa_3=entropy(air,T=Tmix_3, P=Pa_3)
sw_2=entropy(water, T=Tw_2, P=Pw_2)
sw_3=entropy(water,T=Tmix_3, P=Pw_3)
s_prod=m_dot_air*(sa_3-sa_2)+m_dot_w*(sw_3-sw_2)   "Checks 2nd Law"

"4: Combustor Exit"

"Solve for adiabatic flame temperature separate from water injection"

"Balanced stoichiometric reaction:"
{C12H26 + 18.5(O2 + 3.76N2) --> 12CO2 + 13H2O + 69.56N2}

"Complete combustion with varying air-fuel ratios; non-stoichiometric:"
{wC12H26 + x(O2+3.76N2) --> yCO2 + zH2O + qO2 + rN2}
"AF_hat = 1"
w=1
12*w=y
26*w=2*z
2*x=2*y+z+2*q
2*3.76*x=2*r
x = AF_hat/4.76

"Assumed constant air-fuel ratios: 30,50,70,75,80,82,84,86,88,90,92,94,96,98,100%
106.4417857
106.0547619
99.315
94.754
89.276
86.85
83.82833333
80.88714286
79.09333333
76.57833333
74.238
72.61833333
70.99833333
69.225
69.06333333
```

```
66.3525
65.56222222"

"Compute the adiabatic flame temperature without water for each case. Fuel enters at 77 F and air mixture enters at Tmix_3"
"H_products = H_reactants for adiabatic"

"Reactants"
hf = -151538 [Btu/lbmol]
h_O2r = enthalpy(O2,T=Tmix_3)
h_N2r = enthalpy(N2,T=Tmix_3)

"Products"
h_CO2p = enthalpy(CO2, T=Ta_f)
h_H2Op = enthalpy(H2O, T=Ta_f)
h_O2p = enthalpy(O2, T=Ta_f)
h_N2p = enthalpy(N2, T=Ta_f)

hf + x*h_O2r + x*3.76*h_N2r = y*h_CO2p + z*h_H2Op + q*h_O2p + r*h_N2p

Cp_gas = 0.24                                   "Btu/(lbm-F), obtained from generic combustion product gases"
Cp_w = Cp(Water,T=Tmix_3,P=Pw_3)
m_dot_air*Cp_gas*Ta_f + m_dot_w*Cp_w = m_dot_air*Cp_gas*Tmix_4 + m_dot_w*Cp_w*Tmix_4
"Energy balance, finds Tmix_4"

Pa_4 = Pa_3
Pmix_4 = Pa_4 + Pw_4
Pw_4 = y_w*Pmix_4
ha_4 = enthalpy(air,T=Tmix_4)
hw_4 = enthalpy(water,T=Tmix_4, P=Pw_4)
hmix_4 = (m_dot_air*ha_4 + m_dot_w*hw_4)/m_dot_mix

"5: GGT exit"
rp_ggt = 3.02                                   "Used average pressure ratio across ggt from baseline data"
Pa_5 = Pa_4/rp_ggt
Pmix_5 = Pa_5 + Pw_5
Pw_5 = y_w*Pmix_5                               "Need to recalculate water pressures"

W_dot_comp = m_dot_air*(ha_4 - ha_5) + m_dot_w*(hw_4 - hw_5)
ha_5 = enthalpy(air,T=Tmix_5)
hw_5 = enthalpy(water,T=Tmix_5, P=Pw_5)         "Solves for Tmix_5 first, then ha_5 and hw_5"
hmix_5 = (m_dot_air*ha_5 + m_dot_w*hw_5)/m_dot_mix
W_dot_ggt = m_dot_mix*(hmix_4 - hmix_5)         {currently calculated using known temperatures}

sa_5 = entropy(air, T=Tmix_5, P=Pa_5)
sw_5 = entropy(water, T=Tmix_5, P=Pw_5)
smix_5 = (m_dot_air*sa_5 + m_dot_w*sw_5)/m_dot_mix

"6: PT exit"
Pa_6 = 14.03 [psia]                             "Assumed to be slightly less than atmospheric due to vacuum effect of fan"
Pmix_6 = Pa_6 + Pw_6
Pw_6 = y_w*Pmix_6
```

```
smixs_6 = smix_5
smixs_6 = (m_dot_air*sas_6 + m_dot_w*sws_6)/m_dot_mix  {finds isentropic condition}
sas_6 = entropy(air,P=Pa_6,T=Tmixs_6)                  {splits isentropic mixture into components}
sws_6 = entropy(water,P=Pw_6, T=Tmixs_6)

has_6 = enthalpy(air,P=Pa_6,s=sas_6)
hws_6 = enthalpy(water,P=Pw_6,s=sws_6)
hmixs_6 = (m_dot_air*has_6 + m_dot_w*hws_6)/m_dot_mix

eta_pt = (hmix_5 - hmix_6)/(hmix_5 - hmixs_6)          {uses turbine efficiency to calculate actual
enthalpy}
hmix_6 = (m_dot_air*ha_6 + m_dot_w*hw_6)/m_dot_mix
ha_6 = enthalpy(air, T=Tmix_6)
hw_6 = enthalpy(water, P=Pw_6, T=Tmix_6)

"Heat rate and Power"
Q_in = hmix_4 - hmix_3                                 {heat rate during combustion}
Q_dot_in = m_dot_mix*Q_in

W_pt = hmix_5 - hmix_6                                 {work from power turbine}
W_dot_pt = m_dot_mix*W_pt

W_dot_net = W_dot_pt + W_dot_ggt - W_dot_comp

"Water heating energy"
T_supply = ConvertTEMP(C,R,10)
P_tank = 33.5 [psia]
h_supply = enthalpy(water,T=T_supply,P=P_tank)
Q_dot_w = m_dot_w*(hw[2]-h_supply) {this quantity assumed to be provided by a heat exchanger in a
theoretical cycle in order to neglect heating}

"Thermal Efficiency"
eta_th = W_dot_net/Q_dot_in

"Indicated Horsepower (IHP)"
IHP = W_dot_net*3600*convert(Btu/hr,hp)

"Brake horsepower (BHP)"
eta_mech = 0.88 {Obtained from previous gas turbines data}
BHP = IHP*eta_mech

"Brake Specific Fuel Consumption"
{m_dot_fuel = 203.5 [lb/h]} {At 100% throttle}
BSFC = m_dot_fuel/BHP

"Baseline Statistics"
W_net_base = 84.8 [Btu/lbm] {obtained from gas turbines data at 100% throttle}
W_dot_net_base = m_dot_air*W_net_base
W_dot_net_increase = (W_dot_net-W_dot_net_base)/W_dot_net_base * 100
```

Appendix B: Standard Operating Procedures for the Model 250-C20B

To start the engine:

1. Turn on computer.
2. Ensure fuel pump is on and there is fuel pressure
3. Ensure the battery is charged and the power to the dynamometer and control system is turned on.
4. Ensure the water for the water brake is on. Valve should be fully open.
5. Check the turbine oil level.
6. Ensure that the Louvers are open.
7. Check that the fan grating is clear.
8. Turn on exhaust fan.
9. Turn on power at the control bench.
10. Open WinDyn computer program.
11. Place engine control knob to 30%, manual, and med adjustment setting
12. Set dynamometer brake speed to 6000 rpm, and med adjustment setting
13. In WinDyn, select “turbine1” or “turbine2”
14. Turn on Ignition
15. Turn on starter, and hold in.
16. When Gas Generator Turbine speed is at 14,000 rpm, turn on fuel pump. Keep “GGT Temperature” below 1415 F.
17. When GGT speed is 25,000 rpm, turn off starter and ignition.
18. Allow engine to “warm up” for a minute or two before beginning runs.

To stop the engine:

1. Slowly bring engine back down to idle (30% control knob setting)
2. Allow engine to cool off at this setting for a minute or so.
3. Turn off fuel pump.
4. Place engine control knob on 0%.
5. Turn off computer.
6. Turn off fan.
7. Close louvers.
8. Turn off water.
9. Turn off power.
10. Turn off fuel pumps.